ADDIS ABABA UNIVERSITY

ADDIS ABABA INSTITUTE OF TECHNOLOGY

SCHOOL OF MECHANICAL AND INDUSTRIAL ENGINEERING

Rail Vehicle Cab Structural Dynamic Behavior under Collision

and

Improving Its Crush Worthiness

By: Mesay Diriba

A thesis submitted to the school of Graduate studies of Addis Ababa University in partial fulfillment of the requirements for the degree of

Masters of Science in Mechanical Engineering

(Rolling stock Engineering)

Thesis Advisers: - 1. Dr.-Ing. Zewdu Abdi

2. Ato Tollossa Deberie

July-2014

Addis Ababa, Ethiopia

ADDIS ABABA UNIVERSITY

ADDIS ABABA INSTITUTE OF TECHNOLOGY

SCHOOL OF MECHANICAL AND INDUSTRIAL ENGINEERING

Rail Vehicle Cab Structural Dynamic Behavior under Collision

and

Improving Its Crush Worthiness

Submitted By: Mesay Diriba

Approved by Board of Examiners:

Dr.-Ing. Zewdu Abdi.

Advisor ____________________ ____________________

Sign Date

Ato Tollossa Deberie. ____________________ ____________________

Co-Advisor Sign Date

Dr. Daniel Tilahun. ____________________ ____________________

School of chairman Sign Date

Name ____________________ ____________________

External Examiner Sign Date

Name ____________________ ____________________

Internal Examiner Sign Date

ACKNOWLEDGMENTS

God has everything to do. All things were made through him, and nobody was made without him. He is always the sponsor of my existence.

Next I would like to express my sincere gratitude to my advisor, Dr.-Ing. Zewdu Abdi for giving me the opportunity to work on this project. I would also like to express my special gratitude to my Co-advisor Ato Tollossa Deberie for his endogenous support, precise guidance, Critical comments, patience, and encouragement throughout the progress of the project, without him, which this work could have not been completed. He has been a constant source of inspiration throughout my study period.

I would also like to thank Ethiopian Railways Corporation (ERC) for the financial support of my education.

Last but not list, I would like to thank my family specially My Mother *Amsalu* and my lovely brother Mr. Chala (MSc. Student),and my friend Ato Abiy Alene (MSc. Mechanical Eng.) those who are always beside me and played a great role in the completion of this project.

TABLE OF CONTENTS

LIST OF FIGURES

LIST OF TABLES

ABSTRACT

Ethiopia is now constructing a modern and reliable railway industry, consequently; one main problem of the Rail vehicle transportation industry is its accidents. This paper will attempt to develop a passive safety consideration for rail vehicle cab using computational methods for predicting the rail vehicle cab structural dynamic behavior under collision for enhancement in its crush worthiness.

The rail vehicle cab structural dynamic behavior under collision analysis is done for light rail transit (LRT) vehicle cab, through finite element method (FEM) and it is one of the non-linear finite element problems as the vehicle cab structure is the assembly of multiple parts, diverse structural shape and is made of different materials.

During crush, these parts experience high impact loads resulting in high stresses. Once these stresses exceed the material yield load and/or the buckling critical limit, the crashing structural components undergo large progressive elastic-plastic deformation and/or buckling. This system absorbs 4.5MJ kinetic energy in a progressive of 2.25m deformation length. The whole process occurs within very short time durations and this is simulated by non-linear FEM using ANSYS (LS-DYNA).

CHAPTER-1

1. INTRODUCTION

This paper will attempt to develop a passive safety consideration for rail vehicle cab using computational methods by predicting the rail vehicle cab structural dynamic behavior under collision at early design stage and enhancement in its crash worthiness. This is generally concerned with the passive safety of railways passenger transportation systems.

Traditional rail vehicle Cab crash analysis is based on static design criteria where the application of a set of static forces defines the cab structural stiffness requirements under collisions, without considering the structural dynamic effect, by using finite element analysis (FEA), procedure and testing the system for static conditions alone (1).

According to (14) there is a general trend throughout the world to improve the crashworthiness of railway vehicles by passive safety strategies. In the first published paper in 1987, design loads of railway passenger vehicles in Europe and the United States are investigated. By examining UK accident statistics, alternative ways to improve the structural crashworthiness are recommended. General design concept of that proposal is to localize the deformation at the vehicle ends and absorb collision energy in a controlled manner to protect the main passenger survival space. To reach this goal, crush zone systems are designed and examined in Europe and United States and these zones are designed to collapse in a controlled manner during collision and absorb several million joules of kinetic energy.

1.1Background of the Study

The complicated nature of the practical crush processes of rail vehicle makes rail vehicle cab analysis for improving its crash worthiness is done by simulating the structural dynamic behavior under collisions, and this is a very challenging task specially for its non-linearity.(7)

In modern rail vehicle cab crash analysis, Non-linear finite element method is mainly used. This analysis is very important especially at early design stages as it reduces the total number of prototype to be tested practically and, hence; this reduces the production cost and time required for rail vehicle manufacturing process. . Moreover, large scale and highly nonlinear nature of rail vehicle cab structural dynamic simulations make it impractical to conduct direct optimization on the full nonlinear model of the structure; prototype is required to be tested experimentally.

The main objective of this paper is to present a systematic and as considerable as possible a practical methodology to conduct more crush worthy vehicle cab at early design stages by simulating the rail vehicle cab structural dynamic behavior under collision. In the structural dynamic behavior of the rail vehicle cab under collision, the kinetic energy to be absorbed is by ideal plastic deformation of the system component under impact and these crashed vehicle cab components has to be considered as attached to each other after collision(4).

- ❖ The crash process model can be divided into active safety before the collision and passive safety during and after collision (1).

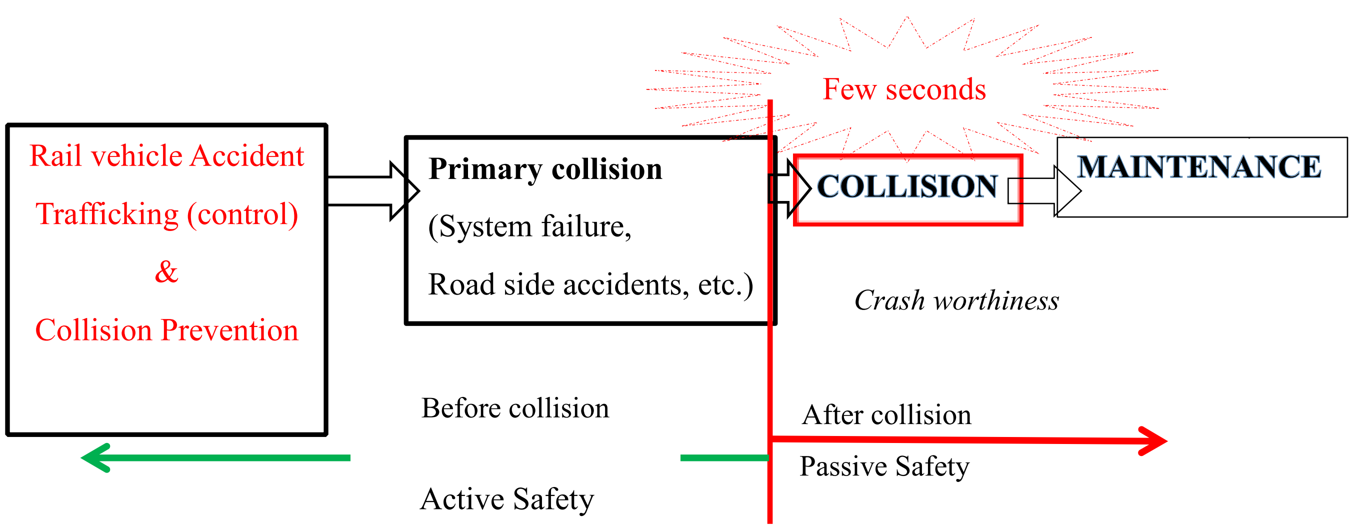

Figure 1-1 Active and passive safety stages for rail vehicle accidents

Active safety is the typical safety of rail vehicle transportation by improved system safety events, and reducing the occurrence of the accidents before collisions.

On the other hand Passive safety is the measure to be taken to present improved safety condition by giving modified passenger protection structure in the event of collisions.

The means by which passenger protection has been done can be categorized by (8):-

1. Maintaining survival space by:
   - Providing a strong survival compartment
   - Reducing crushing Force by using anti-climbers, and providing Cab end structure by crush worthy mechanisms such as pillars.
2. Limiting passenger secondary impact injuries by:
   - Reducing passenger acceleration impulses(using tie belt)
   - Development of furnishings and fittings (i.e. Energy isolation).

The selection of an appropriate energy absorber design (9) relies primarily on the behavior of the structure during the impact (millisecond reaction time) and also the requirements for maintenance of the vehicle after the collision scenarios. This explains that the requirements to be certain that the energy absorber will always perform as designed in the event of a collision, (i.e. ease of inspection and maintenance) and how quickly the maintenance can be made to allow the vehicle to its services.

The collision simulation through Finite element analysis (FEA) for the collision performance of a common energy absorber (3), evaluates the deformation tolerance of the structure, and also allowing for an alternative installation method for ease of assembly and maintenance throughout the vehicle service life.

1.2Railway Accident Statistics and Safety Considerations

Modern railway signaling and train control systems are being developed and adapted with the aim of reducing the number of train collisions. However, it is not possible to prevent all accidents due to internal events such as accidents due to non-functionality of the vehicle system components, and external factors such as level crossing (obstacles or rod vehicles).

The performance of rail vehicles under collision has improved enormously over the last 30 years (1). The passive safety requirements for safety of rail passengers in Europe as an example are described in the legislative European Standards EN 15227: 2008, whose objective is to reduce the consequences of collision accidents. The standard describes the design requirements that railway vehicle bodies should fulfill in order to withstand certain crash conditions, based on the most common accidents and associated risks. One of these design features is the incorporation of energy absorbing devices at either end of the train whose main function is to provide a controlled rate of deceleration of the vehicle in the event of a collision, thereby reducing the impact energy transferred to the vehicle occupants.

Europe rail vehicle accident statistics involving a passenger train between 1991 and 1995 and types of accident are summarized in Table 1-1.

Table 1-1 Accident Distribution in main land Europe (1991-1995) (6)

Accident Type		Number of accidents	%	
Collision between each other	➢ Head on collision	31	10	40%
	➢ Rear collision	69	23	
	➢ Other	21	7	
Collision on Level crossing	❖ Collision with car	28	9	36%
	❖ Collision with lorries/heavy duty truck	80	26	
	❖ Other vehicle	3	1	
Collision not included elsewhere (Others)		24	8	24%
Collision with Buffer stop		33	11	
Collision due to Derailment		2	1	
Derailment without collision		13	4	

This survey led to the development of the following scenarios for consideration for the casualty reduction of Passive safety measures (11):

- ❖ Collision between identical trains at 55 km/h, as this involved the highest number of serious injuries. Identical trains were chosen for ease of definition.
- ❖ Collision of a train with 80 tons UIC buffered wagon at 36 km/h, as trains were prone to overriding in this type of collision. The severity of overriding was highlighted from the

statistics. This scenario also covers buffer collisions, 85% of which were at speeds below 32 km/h.

❖ Collision of a train with a road vehicle (represented by a 16.5 tons rigid block) on a level crossing at 100 km/h. This scenario was considered of particular relevance, as the risk posed is less likely to be reduced by Active safety measures.

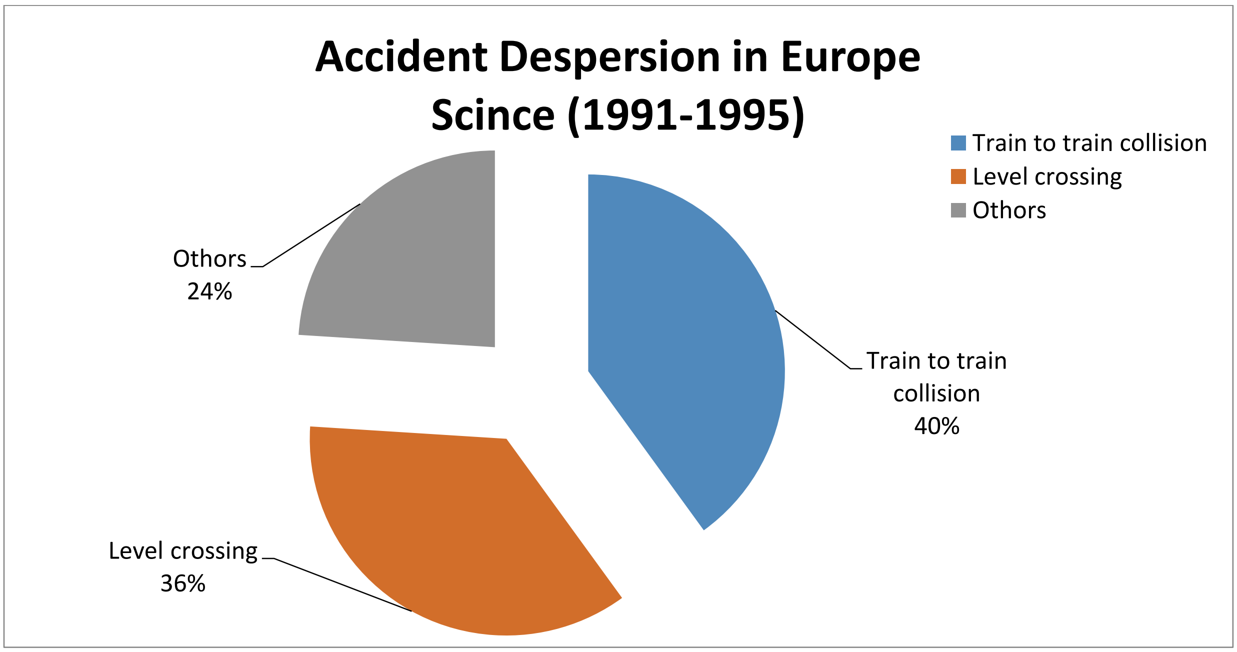

Figure 1-2 Pie chart for Rail Vehicle Accident Distribution in Europe (1991-95)

From the rate of the different collisions scenarios investigated it can be said that the majority is train to train accidents which is 40% which is about two –fifth of the rest. The next is level crossing collisions accidents measures 36% and the remains are mostly train to buffer stop collisions.

1.2.1 Causes of Vehicle Crashes

Different factors contribute to the risk of vehicle collision that may include equipment failure, railway design factors or poor railway maintenance. A behavior of a driver, driver skill and/or weakess and speed of operation are another factor that could lead to vehicle accidents. The vehicle design and road environment are also factors in vehicle collisions (10)

1.3 Statement of the Problem and Motivation

It is known that our country has a long history of railway transportation systems. Due to the fast and sustainability of the economic development, Ethiopia is now under constructing a modern and reliable metric gauge railway industry both light rail transit (LRT) and freight railway transportation industry. Thus, the safety issue of these Rail vehicle transportation systems is the first required activity to reduce the accidents in collisions. This makes this research a feasible and sound. The numerical analysis of the rail vehicle (LRT) structural dynamic behavior in collision provides to select and modify the crash worthiness material improvement. This passive safety design analysis for crash worthiness modification helps to manage the accident due to rail vehicle in collision occurring on practical application.

1.4 Objectives of the Study

In case of design optimization, to evaluate rail vehicle cab structural dynamic behavior under collision, finite element simulation is one of the initial activities in modern rail vehicle design, especially for advancement of crash worthiness. By this design methodology, the entire design life cycle of the system of the rail vehicle structure can be improved under considerable design optimization.

1.4.1 Main Objectives

- ✓ To improve vehicle cab crash worthiness
- ✓ To minimize rail vehicle mass and material cost with more reliability
- ✓ To reduce vehicle running energy consumption (improvement of mass, geometry, material etc.).
- ✓ To optimize performance, space and comfort

1.4.2 Specific Objectives

1. Structurally to Model the rail vehicle cab using Computer aided design software (CAD) (e.g. CATIA V5 R16/19 or AUTO CAD) and computer aided Engineering (CAE).
2. Finite element simulation formulation using ANSYS LS-DYNA for the model to test and simulate numerically the rail vehicle cab for structural dynamic behavior under collisions.

3. To modify (material, geometry) for light rail transit (LRT) especially for improvement of crash worthiness that numerically tested and proposed for new impression.
4. To mention and propose with justification for rail vehicle cab structural requirements for passive safety consideration under collision through controlling its deformation length.
5. To reduce and manage the rail vehicle accidents in a collision.

1.4 Scope and Limitation of the Study

This study is limited to computational finite element analysis alone by using computer aided design (CAD) and computer aided engineering (CAE) software (such as CATIA and ANSYS (LS-DYNA)); from practical perspective it is considerably required to test the prototype experimentally which is very expensive and this is beyond the scope of this paper.

1.5 Application of Results and Benefits

Ethiopian Rail Ways Corporation (ERC) is now structured as a new renaissance of rail way industry of our country; this research will help the design and development strategic plan of millennium goal requirements to manufacture the rail vehicle here in our country. Its importance is mainly for the rail vehicle safety issue by improving structural crash worthiness of the rail vehicle cab, especially for frontal collision. If at the preliminary design stage, the structural dynamic behavior of the rail vehicle cab under collision is numerically simulated and tested for the improvement of its structural crash worthiness; it is advantageous from manufacturing and maintenance cost viewpoint and to reduce the fatality of the accident of the rail vehicle transportation by using optimum and reliable material selection.

1.6 Research Questions

- ❖ How we can investigate the structural dynamic behavior of the rail vehicle cab under collision?
- ❖ How we can model inline Vehicle collision. such as:-
    - I. to the standing vehicle and
    - II. to non-deformable rigid obstacle?
- ❖ What are the methods to be used to modify the rail vehicle cab structure under collision to advance its crush worthiness?

CHAPTER 2

2. LITERATURE REVIEW

2.1 Introduction

In the last two decades, many projects started to improve crashworthiness features of railway vehicles in Europe, United States of America, Japan and India. Starting in 2000, Federal Railways (FRA) in the United States conducted 6 full scale crush tests on passenger cars with and without crash zone systems in 3 different test scenarios: single wagon impact into a rigid wall, two wagons impact into a rigid wall and train to train impact (5).

Following the formation of British Railways in 1948, a number of variants of multiple units and locomotive hauled rolling stock were designed and built. This early Rail vehicle had cab steel frame designed to carry vertical and longitudinal loads and a relatively lightweight steel body which was intended to be non-load carrying (12). According to (13) there were “light” and “heavy” variants of this design under frame with longitudinal proof strengths varying from approximately 110tons to 200tons. The crashworthiness of these vehicles was significantly better than earlier wooden bodied stock, but in collisions involving overriding, the longitudinally stiff vehicle under frame could cause significant damage to the body of an adjacent vehicle.

In the early 1960s another design was developed, this being of a semi-finished steel design and having the ability to carry some longitudinal proof loads above floor level, although not as great as those specified by the international union of Railways (UIC) standards. The crashworthiness of these vehicles was significantly better than that of the previous design because of the higher resistance of the cab body to deformation length and the lower longitudinal stiffness of the under frame. This reduced the susceptibility to, and consequences of, overriding in longitudinal collisions (14).

During the 1970s a new standard design of fabricated steel coach, called the Mk III and multiple unit derivatives were designed and built. These vehicles fully met the longitudinal proof loads for body and under frame as specified in UIC leaflet 566.

Over a number of years following the introduction of Mk III type vehicles it was observed that the performance of the vehicles was very good in a variety of collisions with large amounts of collision energy being absorbed through post yield deformation of the body structure, particularly at the vehicle ends.

During the 1980s British Railways decided to quantify the crashworthiness performance of so called "best current practice" steel bodied Mk III type vehicles, in order that this could be specified for new vehicles. This performance was quantified by performing a longitudinal crushing test on the body ends of a Mark III coach and a Class 317 EMU to measure the force-deflection characteristic of the body ends (cab or rear end) (7).

Following the Electric multiple unit (EMU) crash at Clapham Junction in 1988, British Railways undertook a major crashworthiness development project. This project brought ways of improving and specifying improved vehicle cab structural and interior crashworthiness. A significant influence on this philosophy was the fact that the most common type of collision in Britain was a longitudinal collision between the two trains and most of these collisions had occurred at speeds below 64km/hr.

From the body end crush tests performed on best current practice steel vehicles in the 1980s, it was known that of the order of 1MJ of energy could be absorbed without significantly reducing the survival space within the vehicle.

The philosophy which was developed was that in collisions up to 64km/hr., the kinetic energy of the collision could be absorbed by controlled deformation of the ends of each vehicle within a train, whilst limiting the deceleration experienced by the colliding vehicles.

A requirement of this philosophy is that, in a collision, the couplers between the vehicles involved will retract or break-out during the impact to allow the vehicle ends to engage in order that they can deform and absorb the collision energy.

Upon introduction of Railway Group Standards in the early 1990s, a set of crashworthiness requirements was laid down. These included requirements for 1MJ of structural energy absorption to be provided in a collision between two like vehicles, whilst limiting the collapse distance of a body end to 1m and the collapse force to a maximum of 3000 KN. for multiple units (EMU)and 4000 KN for locomotives and locomotive hauled passenger coaches.

Crashworthiness requirements are currently specified in Railway Group Standard GM/RT2100 Issue 3, October 2000, Structural Requirements for Railway Vehicles.

This issue of the document permits alternatives to the 1MJ of energy absorption per vehicle end providing theoretical simulation is undertaken to determine the required distribution of energy absorption between vehicle ends within the train.

The aim of the literature review reported here has been to gather as much information as possible from worldwide sources on the state of the art of rail vehicle structural dynamic behavior in collisions and improving for crash worthiness. This is to enable a review/comparison of current practice with the latest philosophy and developments worldwide. Research and development projects in Britain, Europe and the USA, have provided a wealth of data, detailed analysis of which is beyond the scope of this search.

2.2Collision Dynamic Modeling Technique

The existing modeling techniques used for collision dynamic analysis can be divided as (15):-

- Lumped Mass Spring (LMS) models (15, 16, 17)
- Finite Element (FE) models (15,16,17)
- Multi Body Dynamics (MBD) models
- Hybrid models

2.2.1 Lumped Mass Spring (LMS) Models

This model is early used in simulating the response of a full rail vehicle in a full frontal impact with a rigid wall (7). The model approximates the structure by a system of lumped masses and springs. The model is quite simple; however, it requires an extensive knowledge and understanding of structural crashworthiness from the user and also a considerable experience in determining the model parameters and translating the output into design data. Moreover, the model also requires that spring parameters to be determined from physical experiments using the static crush setup. LMS models have been used successfully in the simulations of front, side and rear impact vehicle crashes (20)

Limitations of LMS Models

LMS models even though it is valuable to understand the mechanics and the influencing factors of collision such as impact speed, mass ratio and structural stiffness of colliding vehicles. Deceleration time history, amount of energy absorbed by vehicle structure and the amount of deformation can be easily calculated. However, LMS models have its limitations which can be summarized as follows (21)

- It requires knowledge of the spring characteristics of the system under collision, thus it is ineffective for developing new models.
- Highly depends on the modifier experience, skill, and understanding of the crash mechanics.
- For each component 1DOF only limited for predicting the behavior in the longitudinal direction. For example, the behavior due to a misalignment in the horizontal or in the vertical planes cannot be taken. In addition, problems involving offset or angular impact cannot be simulated. Three dimensional LMS models have been developed to overcome this restriction (22, 23).

2.2.2 Finite Element Model (FEM)

Roughly, the history of the finite element starts from the early 1900s, when it was used for elastic bars fields using discrete equivalent formulation (19). As time passed, the finite element method (FEM) has progressed to become the most powerful and complex tool for engineering analysis. The rapid development of the finite element method began as the supercomputers were introduced in the mid 1980’s (24). Understanding the processes behind finite element model analysis with the finite element method starts from the basics of continuum discretization.

The finite element method (FEM) is a numerical method used for solving more difficult engineering problems.. The basic idea is that, the human mind cannot understand the behavior of complex (continuous) physical systems without breaking them down into simpler (discrete) sub-systems. The process of breaking down the continuous system into simpler systems is called discretization and the simpler systems are called finite elements (21).

The standard procedure for the Finite element method has been elaborated over the years and can be summarized as follows:

- ❖ The whole continuous system is discretized into simpler elements of finite sizes interconnected at nodal points.
- ❖ The cause and effect relationship is established over each element. This relation depends on the problem type, e.g., for structural analysis problems, it is a relation between force (cause) and displacement (effect).
- ❖ Equations are assembled (i.e., combining all elements relations) according to continuity considerations and the boundary conditions are applied.
- ❖ The equations are solved using a suitable numerical technique

2.2.3 Non-linear Finite Element Analysis

There are mainly two types of FE analyses (9): linear and non-linear. The main differences between them can be summarized as follows:

In Linear FE analysis, the displacements are assumed to be infinitesimally small, where non-linear FE analysis involves large displacements. The term displacement refers to both linear and rotational motions. In linear FE analysis, the material behavior is assumed to be linearly elastic, whereas in non-linear FE analysis, the material exceeds the elastic limit and/or its behavior in the elastic region is not necessarily linear. Linear FE problems are considerably easy to solve at a low computational cost compared to non-linear FE problems. Also, different load cases and boundary conditions can be scaled and superimposed in linear analyses.

Non-linear FE analysis can be considered as the modeling of real world systems, while linear FE is the idealization one. This idealization can be reasonably satisfactory in some cases, but for special cases non-linear FE modeling is the only option such as in rail vehicle cab structural crashworthiness simulations.

Structural dynamic Simulation of the rail vehicle cab under collision is one of the non-linear problems in mechanical design as it includes all sources of non-linearity.

The sources of nonlinearity can be divided as follows (25).

Geometric non-linearity; -in which the change in geometry is taken into consideration in setting the strain-deformation ($\Delta\varepsilon$-ΔL) relations.

Material non-linearity; that is the material response depends on the current deformation state and possibly past deformation history.

Boundary condition non-linearity; in which the applied force and/or displacement depends on the deformation of the structure.

The whole vehicle cab structure consists of multiple parts with complex geometry and is made of different materials. During crash, these parts experience high impact loads resulting in high stresses. Once these stresses exceed the material yield load and/or the buckling critical limit, the structural components undergo large progressive elastic-plastic deformation and/or buckling. The whole process occurs within very short time durations for these analytical solutions nonlinear FEM is mainly used.

LS-DYNA(2) has been proved to be best suited for modeling non-linear problems such as Simulation for vehicle cab structural dynamic behavior under collision to improve structural crash worthiness.

2.2.4 Multi Body dynamics (MBD) Models

In multi body dynamic models, physical components are represented by interconnecting bodies with different joint types. We can say that LMS models are the special cases of the more general MBD models. The difference is that in MBD models, various joint types with different degrees of freedom can be used and multi bodies can be flexible bodies instead of rigid bodies used in LMS models.

MBD models are efficient at capturing the kinematics and the kinetics of interacting bodies, which is an area best suited for analyzing the response of the human body when interacting with the vehicle interior or vehicle exterior (34) In an early work by McHeny in 1963 (31) he used

MBD to model the human body seated with restraint system in a frontal collision. In his work, the human body is represented by four rigid bodies connected through pin joints. The model was in good agreement with experimental test results.

Currently MBD models are mainly used to simulate the interaction between occupants or obstacles and vehicle structure and also to predict the interacting kinetics between two or more colliding vehicles.

2.2.5 Hybrid Models

A hybrid model combines FE and MBD in a single model. Usually, the FE model is used to simulate the vehicle structure where the MBD model is used to simulate human occupants. This configuration allows for computational efficiency, since MBD can model the human body at a comparatively lower computational cost compared to FE models. LS-DYNA is used to model the vehicle structure and the rigid barrier, where MADYMO, multi body dynamics commercial software is used to model the occupant.

Modeling humans using MBD models has been criticized on the basis that designing a cab based on the dummies responses will make the cab safe for dummies but not necessarily for humans (31). Therefore, research has been conducted in this area to use FE models to model the occupants since they can capture more details about the effect on the body, especially the internal organs. The problem with this approach is the evaluation of material properties for human body parts which is not an easy task.

Moreover, the resulting FE model becomes exceedingly complex and computationally demanding. For example, a human brain model alone consists of more than 300,000 elements (26) Nevertheless, some automobile manufacturers have developed their own FE human models, such as Toyota which has developed Total Human Model for Safety (THUMS) (27)

2.3 Conditions for Structural Dynamic Simulation

The collision dynamics models were designed for a specific set of collision conditions. The applicable scenarios include in-line, frontal collisions with a rigid wall, at speeds up to approximately 50 mph (80.5km/hr.). In these collision scenarios, the damage is expected to be limited to 12-foot (3.7m) vehicle length between the front of the car and the body bolster. The model does not realistically account for structural crushing beyond the front body bolster, but could be modified to do so without much difficulty (4).

The governing equations of motion for dynamic analysis simulation are

- $M\ddot{X} + C\dot{X} + KX = F(t)$ *for transient dynamics(time domain)analysis*
- $M\ddot{X} + C\dot{X} + KX = F_0 Sin\omega t$ *(frequency domain vibration analysis)*
- $M\ddot{X} + KX = 0$ *(also for frequency domain vibration analysis)*
- $KX = 0$*(for static analysis)*

While there was expected to be some vertical and lateral motion in the in-line collisions, the dominant force was expected to be longitudinal. The model can be used to estimate the vertical and lateral motion resulting from in-line, frontal collisions, but it was not meant to be applied in collisions where the principal forces are in the lateral or vertical direction. The model is designed to handle collision forces at the front end of the car, but not from the side or the top. To model side impacts, the model would need to be modified to incorporate impact elements and springs based on the force/crush behavior at the point of impact. Also, the lateral and vertical connection between the trucks and the rail vehicle body would need to be modified to handle the potentially extreme forces between the two masses.

During in-line collisions(3), vertical motion develops when the longitudinal collision forces are offset vertically from the center of gravity (CG) and consequently the Driver's Cab body bounces and pitches on its secondary suspension (29). Due to the long, slender geometry of a rail car, small angles of rotation can lead to significant vertical and lateral forces. Once vertical motion is initiated, it can lead to rail vehicle to override, between colliding Vehicles. The models can be used to estimate the vertical motion during an in-line collision.

Similarly, small vehicle body yaw angles can lead to lateral buckling of the vehicle cab within a train. In the model, small perturbations in the direction of the longitudinal force are used to develop cab body yaw, and hence lateral forces. By discreetly varying the direction of the collision force, the model can be used to bind the range of anticipated lateral motion.

2.4Crushing Elements

The crush zone (9) components that have been developed for a light rail vehicle transit (LRT) cab include coupling system, honeycomb box, the sliding sill mechanism, fixed sill mechanism, primary energy absorber, roof energy absorbers, integrated end frame and anti-climber elements(3).

1. *Honeycomb box:* Honeycomb box composed of the buffer beam, the buffer support, the shear bolts and the aluminum honeycomb block. Two honeycomb boxes are placed on the wagon, one on each side of the centerline of the rail vehicle. When the impact force push the coupling to back and the ends of coupled cars come into contact through the anti-climbers, at the defined load, the shearing bolts between buffer beam and support plate will be cut and buffer beam will crush the honeycomb block.

2. *The sliding sill mechanism*: The sliding sill provides a guide for the end crush zone of the rail vehicle. It consists of U shaped beams sliding within guide channels. It is attached to the fixed sill through the shear bolts. After the honeycomb box is activated, the load at the end frame rises, and the sliding sill shear bolts fracture when the impact load reaches to a defined load.
3. *Primary energy absorber*: Two primary energy absorbers are on the rail vehicle, one on each side of the centerline of the car and consist of six pyramidal thin walled tubes having different lengths. Each absorber is welded to and supported by the car structure that is not intended to deform. The load on the outboard ends of the primary energy absorbers is applied by the back of the support plate. An initial gap exists between the outboard end of the absorber and the back of the buffer beam before activation of the crush zone (so that the absorbers do not carry operational loads).
4. *Roof energy absorbers:* Two roof absorber assemblies are on the rail vehicle located one on each side. They consist of tubes that riveted to each other and contain aluminum honeycomb cartridges. When the load at the roof absorber reaches to a defined load, the rivets shear and the tube pushes back against the honeycomb pieces.
5. *Integrated end frame*: The integrated end frame was designed to remain sufficiently stiff in transmitting the impact load to the energy absorbers, ensuring the proper functioning of the crush zone elements. The integrating end frame can appropriately trigger and allow

crushing of energy absorbers when the coupling and anti-climber share the impact loads or when the lead path is only through the coupling or the anti-climber.

6. Anti-climber: In order to prevent the climbing of two interacting vehicles during a collision, a ribbed anti-climber element is mounted on the end of the under frame over the coupling. No energy absorption is associated with the anti-climber element.

2.4.1 Improving for Crashworthiness

Crashworthiness is the process of improving the crash performance of a structure by scarifying it under impact for the purpose of protecting occupants from injuries. To improve the structural design for crashworthiness, it is required to understand the different factors affecting the crash process.

Accidents occur in an arbitrary mode. A rail vehicle can be impacted from any direction at different speed. According to *Galganski (6)*, crashworthiness problems can be characterized by:

Displacement and energy: Frontal structure length is being reduced by modern design styles and at the same time, it is required to absorb most of the impact energy and to minimize interruption into the compartment.

Crash pulse: Crash pulse is the deceleration induced by impact on the human body. Head injury criterion (HIC) is used to measure the damage from crash pulse on the brain, and it should be less than a certain limit by regulations.

Crash position: The structure should be able to mitigate injuries in different crash positions such as full frontal impact, offset frontal impact, side impact, rear impact, and rollover.

2.4.2 Developing Energy Absorbing Element /Material and Geometry

By definition, crashworthiness is the measure of the structure's ability to protect the occupants during impact; therefore the structure must fulfill some requirements:

- It must absorb as much impact energy as possible by plastically deforming in a controllable manner to minimize the remaining impact energy which can then be handled by the restraint system (7).

- The structure must preserve at least the minimum survival space to keep injury and fatality levels as low as possible.

A good design should achieve these two objectives simultaneously and at the same time, it must adhere to other design aims, e.g., comfortably, accessibility, weight, energy consumption...etc. Thus, the full design process is very complicated and requires high levels of communication between different disciplines.

As the special operation conditions for the rail vehicles driver's cab the following requirements should have to be formulated for crashing elements.

- High energy absorption capability
- Predictable and reliable deformation
- Low production cost
- Maintenance free
- Easy to replace or easily restore after operation

For the cab structural Component modification, in depth individual part simulation is required to verify that each component deformation has to be in required manner. The complete rail vehicle cab model should be then built according to the assembly drawings used for the integration of the effect of crush energy and damping efficiencies of the assembly.

		Aluminium plate	Aluminium honeycomb
Density (kg/m^3)		2770	49.6
Young's Modulus (MPa)	z-dir (axial)	71000	517
	x-dir (lateral)		5.17
	y-dir (vertical)		5.17
Poisson's Ratio		0.33	0.05
Shear Modulus (MPa)	XZ	26000	310.3
	YZ		151.7
	XY		2.3
Compressive Yield Strength (MPa)		280	0.9

Table 1: Material properties of aluminium plate and honeycomb used in finite element model.

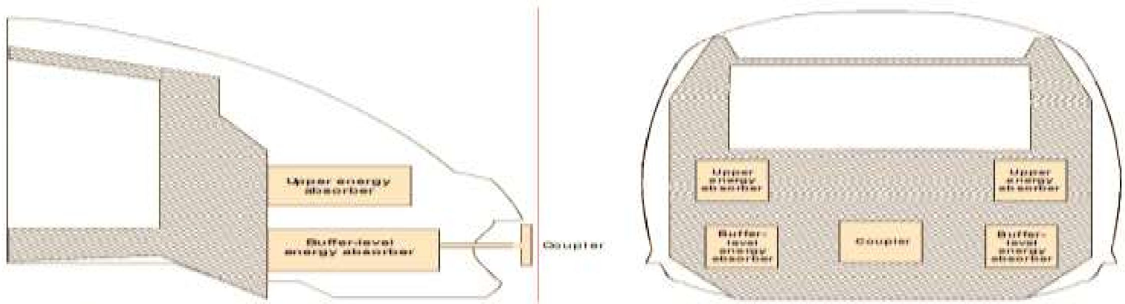

Figure 2-1 Rail vehicles Structural and Material Model for Crashing Element (13)

Generally as a conclusion, there were a Significant research projects on rail vehicle passive safety consideration, specifically on frontal impact structural dynamic behavior under collision for modification in its crash worthiness, have been undertaken in recent years, particularly in Europe and the USA. These design simulations at early stage on structural dynamic behaviors in collision have been aimed at reducing human life and material losses in rail vehicle accidents by improving structural crashworthiness of the rail vehicle structure.

As the result of our country, Ethiopia is aimed to develop a new and modern Rail way industry, a review of this research is of particular relevance to the future design and development of rolling stock of our country. Also, a major non-linear FEM of analysis and testing has been led by other Country for Rail way industry and the knowledge gained from this work should be included, where applicable, in the development of an enhanced dynamic behavior in collision and improving for crash worthiness specification for Ethiopian railway vehicles.

CHAPTER-3

3. RESEARCH METHODS, MATERIALS AND PROCEDURES

3.1 Research Methods

The following procedures have been used to realize the objectives of this research. Figure 3-1 Modeling Methodologies in impact analysis shows that how the model process has been broken down into various stages of essential analysis.

The finite element model evaluates the various modes of deformation that occur during impact and determines the load path.

The force-crush behavior of the system is then used as an input for collision dynamics model analysis. The model produces the gross motions of the cab bodies and timing of events. The collision dynamics model supplies a three-dimensional crash pulse for the interior occupant models. These models generate the secondary motions experienced by the occupant seating arrangements. These three models are then developed to simulate the impact energy and the structural response of the cab for enhancing its crush worthiness.

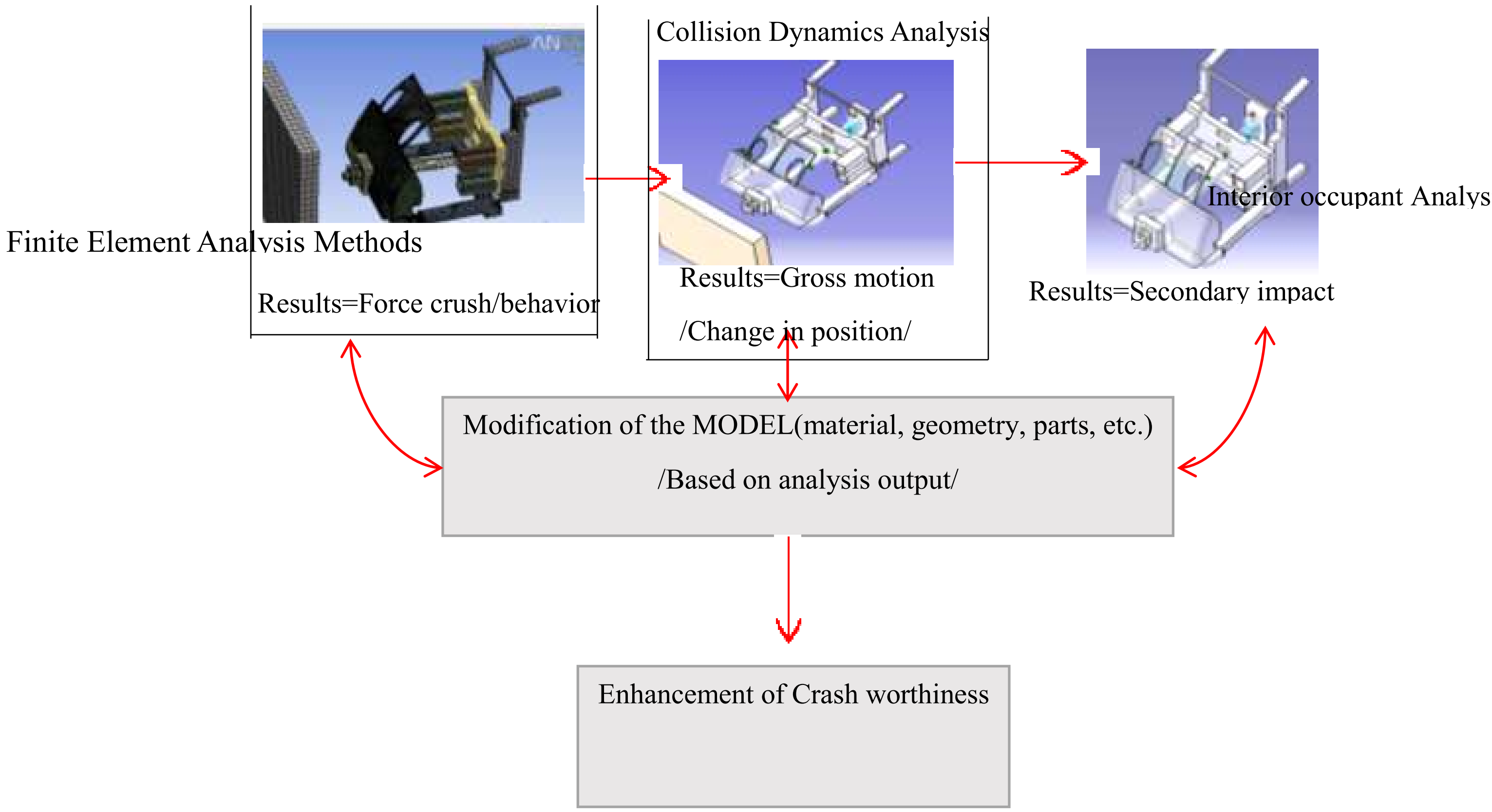

Figure 3-1 Modeling Methodologies in impact analysis

3.2 Computational Analysis Process Methodology

3.2.1 Cab3D Modeling Procedure

Under this activity the author uses CATIA V5 (R16/orR19) 3D modeling for standard rail vehicle dimensions of LRT. CATIA is one of the most CAD software that enables to model especially for its 3D model feature applications such as part design, and assembly design workbenches. CATIA (computer aided three dimensional interactive application) uses a Dassault Systemes computer language system as such of solid work and ABAQUS software.

3.2.2 Proposed System Specifications

Table 3-1 Light Rail Transit (LRT) Cab Design specifications

Specification	**Value**	
Track Gauge(standard)	1.435m	
Vehicle weight(Empty, average)	41000kg	
Vehicle weight(Full, average)	63000kg	
Single vehicle Height(with pantograph)	3.9m	
Single vehicle length(average)	28m	
Single Vehicle width	2.65m	
Horizontal vehicle clearance(total)	1.0m	
Vertical vehicle clearance(minimum)	4.1m	
Ballast/Track bed depth (average)	0.74m	
Passengers (seated/standing, total)	60/130, 190	
Maximum Operation speed	120km/hr.	
Emergency brake distance on straight line (with 30% over load and initial speed 120km/hr.)	≤800m	
Minimum negotiable curve	Single car	100m
	Coupling	145m
Ride index	W≤2.5	
Noise Level (120km/hr.)	≤68dB(A)	
Axle Load	≤17t	

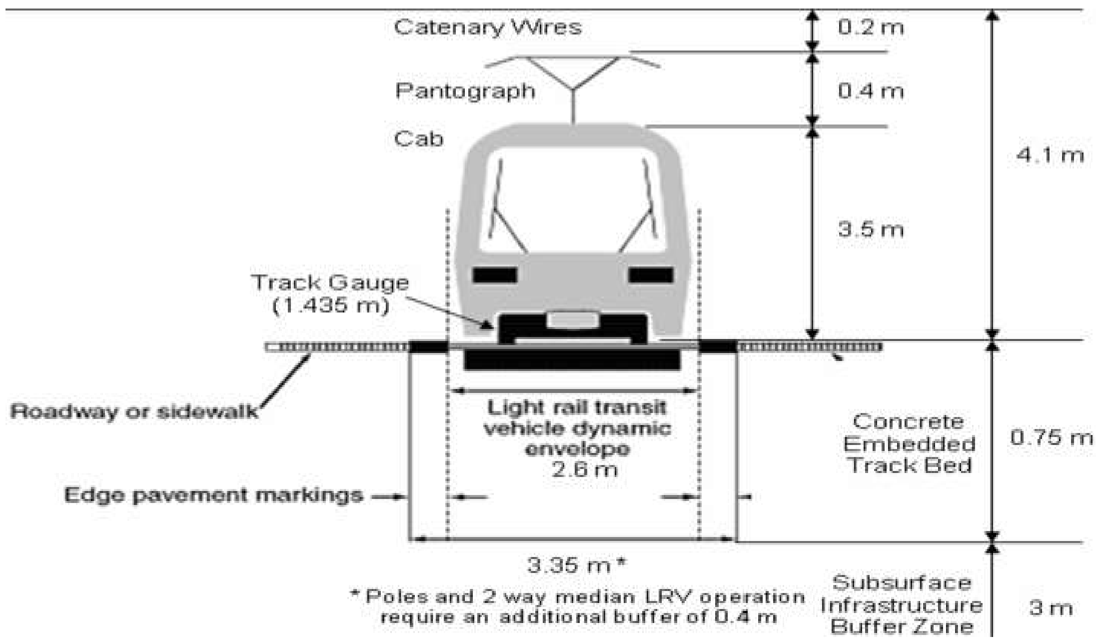

Figure 3-2.Light Rail Transit (LRT) Over All Dimensions (14)

Then the 3Dmodel is saved as ANSYS LS-DYNA format for structural dynamic simulation by nonlinear FEM computation.

3.3 Cab Crashing Element and 3D Modeling

3.3.1 Structural Components

a. Supporting Pillars

The main structural components of the existing Rail vehicle cab are two substantial welded steel supporting pillars. These provide much of the cab's overall static stiffness and strength. They also resist the collapse loads of the energy absorption devices such as upper and lower energy absorber.

b. Cab shell (Body shell)

Cab shell is a thin composite sheet metal which is attached to a steel-sub frame. The profile of the rail vehicle Driver's side is one of the factors for aerodynamic effect of the vehicle. The cab structure and ineffective use of space requirement of the cab shell result in poor energy absorption capacity in collisions.

c. Upper energy Absorbers

The upper energy absorbers are welded to the rear bulkhead (i.e. the steel plates that is directly welded to the supporting pillars). This structure absorbs the main impact energy through its deformation length.

d. Primary(main) energy Absorber

Behind the nose is the main crush zone that houses the primary energy absorbing devices for compliance with EN 15227 standard. This is a self-contained module that can be removed and replaced if necessary.

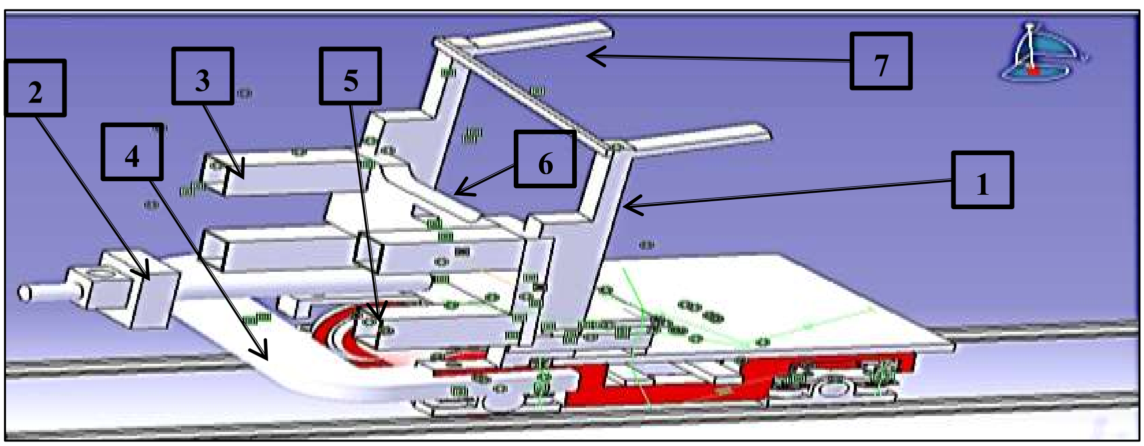

1. Supporting Pillars **4. Anti-Climber Energy Absorber**
2. Main (Primary) Energy Absorber
5. Lower Energy Absorber ***6. Honeycomb* Plate**
3. Upper Energy Absorber
7. Roof

Figure 3-3 Main structural components of the Rail vehicle Driver's Cab

e. Aluminum honeycomb absorber

Aluminum honeycomb absorber is a plate that joins the supporting pillars. The honeycomb box is composed of the buffer beam, the buffer support, the shear bolts and the aluminum honeycomb supporting pillars. Two honeycomb boxes are placed on the wagon, one on each side of the centerline of the car. When the impact force push the coupling to back and the ends of coupled cars come into contact through the anti-climbers, at the defined load, the shearing bolts between buffer beam and support plate will be cut and buffer beam will crush the honeycomb block i.e. supporting pillars.

f. Lower energy Absorber

Lower energy Absorber are large aluminum tube which are a blocks of aluminum honeycomb of varying density as required. During crush this structure begins crushing at rear part (lower density) rather at impact position by self-aligning deformation procedure.

g. Anti-climber Energy Absorber

Anti-climber Energy Absorber is a cab lower part that provides for removal of the objects on the rail. In order to prevent the climbing of two interacting vehicles during a collision, a ribbed anti-climber element is mounted on the end of the under frame over the coupling. As a standard requirement no energy absorption specification is associated with the anti-climber element.

h. Cab Nose

The rail vehicle cab nose section, which is the area most likely to suffer incidental damage, has been designed to be easily removable for maintenance or replacement. Removing the nose also provides easy access to the primary energy absorbing devices for inspection or replacement purposes.

i. Fiber Glass

The glass fibers, polystyrene resin and polyurethane foam were then laid-up inside the cab shell determine and allowed to cure before securement. This is an optical glass which allows seeing and controlling of the Locomotive during operations.

j. Roof

The roof energy absorbers are the two connected on upper end of each supporting pillars of the car located one on each side. They consist of tubes that riveted to each other and contain aluminum honeycomb cartridges. When the load at the roof absorber reaches to a defined load, the rivets shear and the tube pushes back against the honeycomb pieces. The energy absorption capacity of the roof energy absorbers is 0.02 MJ and the stroke is 25 cm.

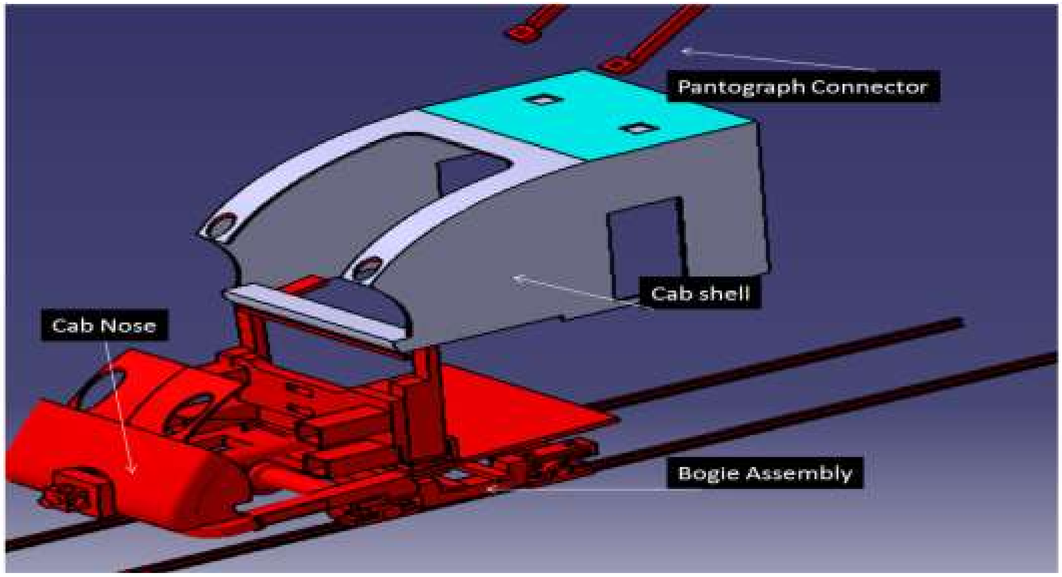

Figure 3-4 Minor Energy Absorber (Cab nose and Cab shell)

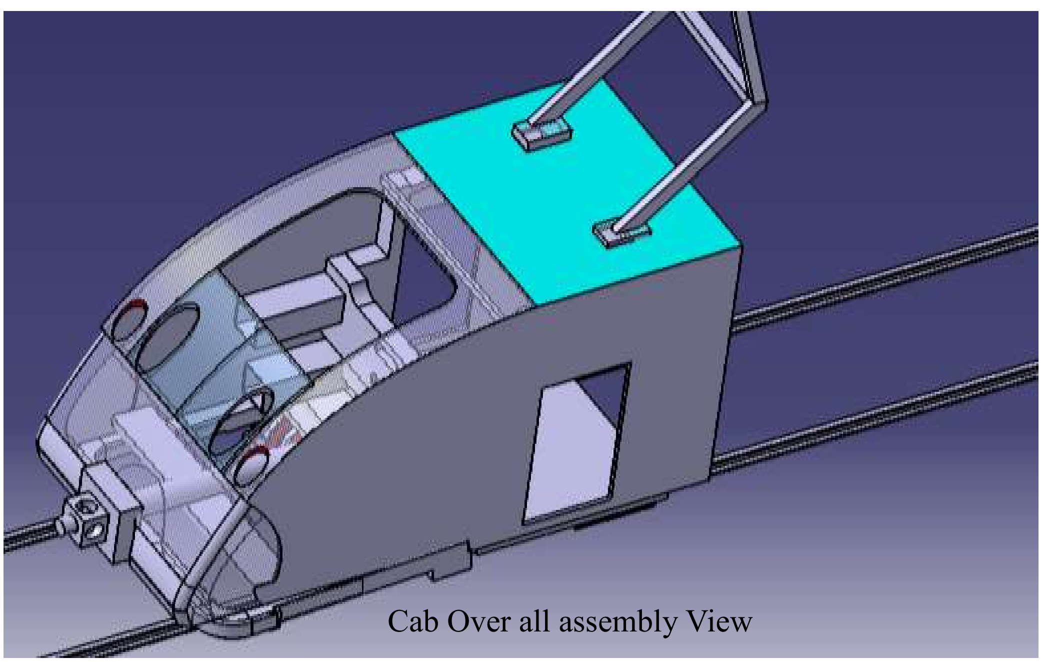

Figure 3-5 CATIA 3DModel for Finite element Analysis

3.4 Cab Structural Crushing Zones

- Primary Crush Zone

This frontal structure cab nose, Anti-climber, some part of main energy absorber and which is required to have detachable nosecone and easy for Replaceable, absorbs the crush energy more than0. 2MJ to meet some standard crashworthiness requirements

- Secondary crush Zone

This are the main energy absorption structure which consist of both upper and lower energy absorbers, as well as main energy absorber for buffer level impacts conditions.

- Reaction Zone

These are the cab structures specially supporting pillars and honey comb structure which are more rigid and non-deformable parts that used for load path rather than deforming during collisions.

3.5 Process of Collision and Its Effect

The process of the rail vehicle collision can be investigated at different stage: These are:

- Pre-crash process,

During pre-crash processes the effect of the braking system, the normal train and traffic controls systems, the vehicle diagnostic systems, in general, the factors of Active Safety systems problems clearly distinguished.

- primary collision

This means that the impact of the vehicle to any ambient objects, such as collision between each vehicle or to a buffer stops. The consequent or result of the primary crash is the rectilinear deceleration/acceleration of the vehicle. Overriding of under frames, jack-knifing of the vehicles, overriding, sliding, and impacts again are the output of the primary collision.

- secondary collision

Secondary collision is the impact of the passengers to the passenger seat or any vehicle internal objects. There are two types of secondary impact to be distinguished.

1. Impact due to crash of the passenger seat

During collision the vehicle body deforms to a high degree, so the occupant space may not remain enough survival space for the passenger. Thus there is a high impact of the occupants to the vehicle internal structure.

2. Impact due to relative speed difference between the passengers and the vehicle body

   As a result of the relative speed difference between the passengers and the vehicles results in the passenger impact to the vehicle body, to interior equipment or eventually to another person, but the inner space doesn't decrease dangerously.

- post-crash process

Post-crash process is the result after the collision may be fire, explosion and outflow of dangerous materials that can occur. These problems belong to another field of vehicle engineering.

3.6 Crash Component Performance Measures

3.6.1 Interior Occupant Performance Measures

The occupant head injury criteria (HIC) have been most widely used to assess severity and thus the injury risk of vehicle crashes. The HIC relates to acceleration of the occupant head over a continuous duration of 36ms, 15ms and is often denoted as HIC15 (13).

There were lots of medical and biomechanical researches carried out to determine the endurance limit of the human body. On the experiments several injury criteria were established to certain parts of the body. For instance in the beginning in case of head impacts the acceleration of the center of mass was simply integrated with respect to time using the following equation. Later on the formula was modified in accordance with the observation.

$$\boldsymbol{HIC} = \left\{\left[\frac{1}{t2-t1}\int_{t1}^{t2} \boldsymbol{a(t)dt}\right]^{2.5} * (\boldsymbol{t2}-\boldsymbol{t1})\right\} \quad \textbf{3-1}$$

Where *a (t)* is the head deceleration measured in m/s^2 and (*t2-t1*) defines the duration of the acceleration event, which is limited to 36ms, 15ms. The HIC15 measure is thus computed over several 15ms intervals within the acceleration-time history of the impact response. The current crash safety regulations state that the peak HIC15 value over a continuous 15ms interval should not exceed 700 (14).The European Union Road Federation (ERF) (15) has further defined an abbreviated injury index scale (AIS) as an exponential function of the HIC. The study proposed an AIS threshold of 1.5 for minimal injury that corresponds to HIC15 of 350. It was found that AIS is exponentially proportional to the occupant HIC after the AIS threshold value (16)

Table 3-2 Injury criteria for certain parts of the human body (from US Department of transport)

Human body	Type of force	Maximum
Head	$HIC_{36}(t_2-t_1=36ms)$	<1000
	$HIC_{15}(t_2-t_1=15ms)$	<700
Neck	Tension force	<4170N
	Compression force	<4000N
Thorax	Acceleration(T_{max}=3ms)	<60.g
	Deformation	<76mm
Pelvis	Acceleration(T_{max}=3ms)	<80.g
	Angular displacement	$<20^0$
Hip joint	Tension force	<12.5KN
Thigh (bone)	Axial force	<10KN
Leg (bone)	Axial force	<1KN

3.6.2 Specific Deformation Length (μ_d)

The vehicle deformation, expressed by maximum dynamic crush of the frontal structure, has been greatly associated with the degree of occupant compartment intrusion. The specific deformation magnitude is defined as the ratio between maximum deformations, (L_c) $_{max}$, to the vehicle total length (L), i.e.

$$\mu d = \frac{(Lc)\ max}{L} \qquad 3\text{-}2$$

Where μ_d is the specific deformation magnitude that describes the degree of total crushing rate and it could be used as an indication of the degree of compartment intrusion. The frontal vehicle structure should not be allowed to deform more than certain value, which is usually less than 0.65. A deformation beyond this value will cause an intrusion into the occupant compartment. In this study, since the overall cab length of the lumped-parameter model is unknown, the total deformation is used for measuring the compartment intrusion.

3.7 Finite Element Models for Collision Dynamics Analysis

The finite element method analysis of the model makes the initial indication of the cab assembly deformation by force-crush behavior. Here, a methodology for enabling an efficient and effective procedures for rail vehicle cab structural dynamic behavior analysis under impact and improving its crash worthiness have been proposed as follows.

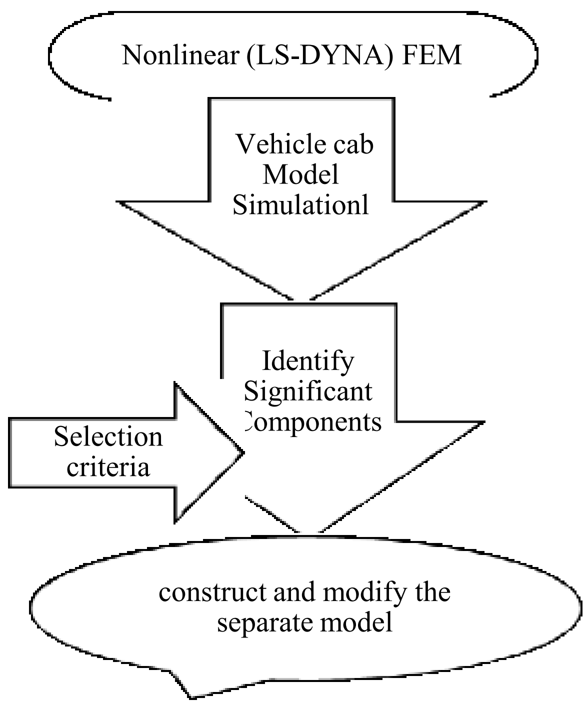

Figure 3-6 Finite Element Models Flow Diagrams

FEM computational analysis procedures

- Define the vehicle characteristics(speed, mass) to use as input data
- Define the collision scenarios
- For the model simulate the analysis using ANSYS LS-DYNA software
- Collect the data generated from the dynamic simulation and examine the results; and
- Formulate and justify for design optimization.

3.8 Over View of ANSYS LS-DYNA Software

ANSYS LS-DYNA is a nonlinear transient dynamic finite element code (program) that planned to solve short duration dynamic problems. ANSYS LS-DYNA technology is the result of collaborative effort between *ANSYS, Inc*. and *Livermore software Technology corp. (LSTC)* of USA. It introduced in 1996, and can analyze large deformation behavior in structures by the explicit time integration method.

LS-DYNA has been developed in California for more than 20 years. It is the most frequently-used code for many complex applications in structural nonlinear dynamics (39).

Its usage is growing rapidly due to LS-DYNA's flexibility, enabling it to be applied to new disciplines. The new developments are driven in co-operation with leading universities from all over the world and new requirements requested by the vast customer base. It is widely used in crush worthiness analysis, earthquake Engineering, Metal forming, drop test of electronics (cell phone) impact analysis, etc.

LS-DYNA was originally developed for military purposes to model blows of bombs but rapidly was used in several fields. Explicit finite element method is widely used in analysis of phenomena of energy absorbing. Due to its large capabilities in a field of highly nonlinear and very short term actions it is one of the main tool in designing either whole vehicle wagon or particular energy absorbing elements.

Another advantage is a detailed material library with damage models of almost all materials used in construction such as metals, composites and foams.

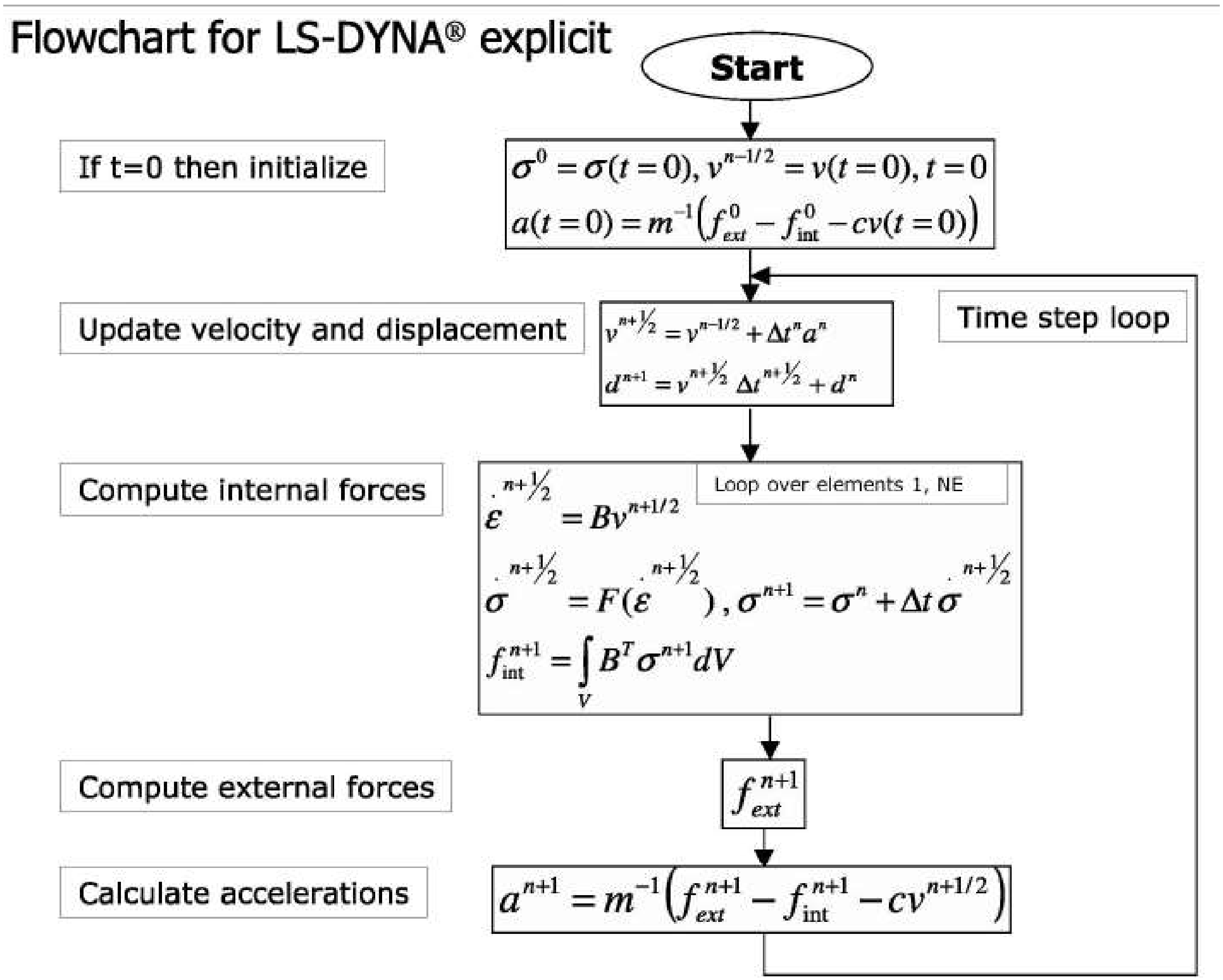

Figure 3-7 Explicit LS-DYNA flowchart (41)

CHAPTER-4

4 FINITE ELEMENT MODEL

4.1 Introduction

The principle of virtual work can be used to derive the governing differential equations in finite element model which states that the work done by external loads is equal to the work done by internal loads. It should be noted that the principle of virtual work can be applied to both linear and non-linear problems.

Now, applying the principle of virtual work to a finite element with elemental volume (V_e), we can formulate as:-

Work done by Internal Force=Work done by External Force

$$\Delta\,(U_{int.})_{eV}=\Delta\,(W_{ext.})_{ev} \quad \text{4-1}$$

Where, $\Delta\,(U_{int.})_{ev}$ is rate of work done by internal force on elemental volume.

$\Delta\,(W_{ext.})_{ev}$ is work done by external force on an elemental volume

Spatial approximation using the finite element method and time approximation where the ordinary differential equations are further approximated in time are computed by reaching the dynamic equilibrium equation at the end of every time step. Considering $\{X\}$ as the displacement nodal values vector, $\{\dot{X}\}$ as the nodal velocities vector and $\{\ddot{X}\}$ as the nodal acceleration vector, the dynamic equilibrium equation is computed at the end of every time step and has the following formulation:-

$M\ddot{X}+C\dot{X}+F_{int.}=F_{ext}$

$$[M]\{\ddot{X}\}+[C]\{\dot{X}\}+[K]\{X\}=\{F_{ext.}\}(t) \quad \text{4-2}$$

Where $\{\ddot{X}\}$, $\{\dot{X}\}$ and $\{X\}$ are $m \times 1$ vectors, [M] is the $m \times m$ system mass matrix, [C] is the $m \times m$ damping matrix, [K] is the $m \times m$ stiffness matrix and $\{F_{ext}\}$ is the $m \times 1$ total forces vector, while m is the number of nodal degrees of freedom per finite element model.

4.2 Explicit Dynamic Analysis

Crash analysis requires a dynamic analysis formulation (body movements) and a non-linear transient dynamic explicit type of finite element analysis. A non-linear dependency describes the relation between the applied conditions and resulting effects (e.g. surfaces in contact change in time or large deformations of metal parts). Therefore, a non-linear investigation is required in crash analysis, since large amounts of plastic deformation occur in most crash scenarios. Transient (with time integration) analysis is a type where the movement and body deformations are time dependent. In crash situations, the time frame is short and the analysis is highly dynamic. The explicit formulation of finite element analysis is a specific mathematical approach that mostly used for high velocity, short time frame circumstances.

Explicit Finite Element Method has been found as outstanding tool to solve complex tasks that include large deformations of structures, great inertia effects and analysis of contact is developed in several algorithms which make it much easier to perform and control the response than in implicit solvers. Explicit Finite Element Method is based on *Central Difference Method*. Nowadays, explicit non-linear finite element method is widely used for simulation of high speed events, especially in Rail vehicle crash testing condition. The equations of motion for *linear behavior* collision give the linear ordinary differential equation.

For some linear ordinary differential equation of motion closed form solutions are possible but for most of non-linear equation, only numerical solutions are the only choice to solve.
Numerical analysis, in general, tries to solve the mathematical problems like differential equations by numerical procedures. The differential equation can be split into numerical components in the time axis using the forward, central or the backward differentiation methods. The numerical methods also can be broadly classified as the *explicit* and *the implicit* methods. The explicit method calculates the next time step value using the previous time step values, whereas the implicit method calculates the next time step values by solving a matrix of the present and the previous time step values.

The explicit method requires shorter time step for an accurate solution, whereas the implicit methods can give reliable results with larger time steps. Also, most of the implicit methods are unconditionally stable, whereas the explicit methods are mostly conditionally stable. In implicit method contact cannot be easily controlled. Hence this method is not used for crush simulation. While the equations for the *non-linear* behavior give the internal force as a non-linear function of the displacement leading *to non-linear* ordinary differential equation of motion.

$[M]\{\ddot{X}\}+[C]\{\dot{X}\} + \{F_{internal}(x)\} =\{F_{ext.}(t)\}$.. 4-3

Where, $\{F_{internal}(x)\} = [K]\{X\}$ Represents the internal forces resulting from the plastic deformation of a structural part

$F_{ext.}(t)$, is the external nodal load vector

Re-arranging this equation of motion at any t_n is then given by:-

$M\ddot{X}= -C\dot{X}- F_{internal}(x) + F_{external}(t)$

To advance the equations in time t_{n+1}, LS-DYNA uses the central time integration.

$\ddot{X}_n=M^{-1}(F_{ext.}(t)_n -C\dot{X}_n- F_{internal}(x)_n)$

i.e. $\ddot{X}_n= [M]^{-1}(F_{ext.}-F_{int.})_n$.. 4-4

Where the mass matrix [M] is diagonalized for fast inversion (if it is not already diagonal) by specific mathematical algorithms, creating a lumped mass matrix, Stiffness or damping (if considered) matrix inversion are not required. Stiffness and damping effects are included in the internal force vector $(F_{int.})_n$

4.2.1 Hour-glassing Effects

Hour-glassing is a zero-energy mode of deformation that oscillates at a frequency much higher than the structure's global response. Hour-glassing modes result in stable mathematical states that are not physically possible. They typically have no stiffness and give a zigzag deformation appearance to a mesh. Single point (reduced) integration elements are lying to zero energy modes. The occurrence of hour-glass deformations in an analysis can invalidate results and should always be minimized or eliminated. If the overall hourglass energy is more than10% of the internal energy of a model, there is likely a problem with the analysis. Even 5% can be considered excessive, in some cases.

$$\mathbf{F_{int.} = \Sigma(\int_V B^T \sigma_n dV + F_{hg}) + F_{cont.}} \quad \textbf{4-5}$$

Where, F_{hg} is the hourglass resistance force and $F_{cont.}$, is the contact force.

Methods in Minimizing hour-glassing in ANSYS LS-DYNA

- Avoid single point loads, which are known to excite hourglass modes.

Since one excited element transfers the mode to its neighbors, point loads should not be applied. Try to apply loads over several elements as pressures, if possible.

- Refining the mesh often reduces hourglass energy, but a larger model corresponds to increased solution time and larger results files.
- Use fully integrated elements, which do not experience hour-glassing modes. However, penalties in solution speed, robustness, and even accuracy may result, depending on the application.

In crash analysis with explicit analysis method, equation (5-3) is integrated in time domain by applying certain simplifications. The resulting mathematical expression is solved every time step:

$$\{\ddot{X}\}=[M]^{-1}\{F_{ext.}-F_{int.}\}$$

Generally an explicit dynamics analysis is used to determine the dynamic response of structure due to stress wave propagation, impact or rapidly changing time-dependent loads. This type of analysis can be used to model mechanical phenomenon such as rail vehicle cab crash analysis which are highly non-linear.

4.2.2 The Source of Non-linearity

- Material

Non-linearity may result from *material* response to the collision energy as a result of hyper elasticity disorders, plastic flows, and failure conditions which is material dependent.

- Contact

Due to high speed collisions and the structural response under impact energy at contact can result in non-linear response under the impact durations.

- Geometry

One of the sources of Non-linearity may result from *geometric deformation* such as buckling and collapse.

Newmark's algorithm is a mathematical routine generally used in dynamic analysis (6). The scheme approximates displacements, velocities and accelerations at time step *n+1* by using the following routine.

$\{X_{n+1}\}=\{X_n\}+\Delta t\{\dot{X}_n\}+1/2(1-\beta_2)\,\Delta t^2\{\ddot{X}_n\}+1/2\,\beta_2\Delta t^2\{\ddot{X}_{n+1}\}$

$\{\dot{X}_{n+1}\}=\{\dot{X}_n\}+(1-\beta_1)\Delta t\,\{\ddot{X}_n\}+\beta_1\Delta t\,\{\ddot{X}_{n+1}\}$

Where β_1 and β_2 are Newmark's constants and Δt is the analysis time step. The values given to Newmark's constants reduce the equations to either an implicit, either an explicit routine.
The explicit equations are obtained by setting $\beta 1$=1/2 and $\beta 2$=0. Consequently, the explicit time integration algorithm becomes.

$\{X_{n+1}\}=\{X_n\}+\Delta t\,\{\dot{X}_n\}+1/2\Delta t^2\,\{\ddot{X}_n\}$

$\{\dot{X}n_{+1}\}=\{\dot{X}_n\}+1/2\Delta t\,\{\ddot{X}_n\}+1/2\Delta t\,\{\ddot{X}_{n+1}\}$

Most finite element analysis solvers based on the explicit algorithm adapted the Newmark scheme into a staggered time marching routine, in which the nodal velocities are computed at half time steps$\{\dot{X}n_{+1/2}\}$ and displacements at full time steps$\{Xn_{+1}\}$ (12). The integration algorithm is referred to as the central difference routine:

$\{\dot{X}_{n+1/2}\}=\{\dot{X}_{n-1/2}\}+\Delta t_n\,\{\ddot{X}_n\}$.. **4-6**

$\{X_{n+1}\}=\{X_n\}+(\Delta t_{n+1/2})\,\{\dot{X}_{n+1/2}\}$.. **4-7**

Looking at the explicit routine equations, it is observed that the information at time step *n+1* is obtained by using only the information from the previous step. The character of the algorithm by directly obtaining the present information from previous known data, without the necessity of equations solving (as implicit schemes require), gives its name, i.e. explicit formulation.
Numerical stability is maintained by choosing a small time step *Δt*. If the time step is over-much small, the solution will require long computational time, generally with little to no improvements in accuracy. On the other hand, if the time step is too large (exceeding the minimum time step size), the solution calculation may fail because of divergence. Consequently, there must be a

maximum value of the time step at which the solution can reach convergence. The integration time step **Δt** must satisfy the Courant condition (4, 5)

$$\Delta t = \frac{Lc}{C}$$

Where L_C is the smallest characteristic length of all the elements in this method the size of the time step is related to the size of the smallest element L and C is the speed of sound in the material. The critical time step ($\Delta t_{critical}$) is the condition that when the computation should not advance faster than a physical phenomenon. It depends on the density and the Young's modulus. The explicit analysis requires a small time step (around 1 msec.) which leads to a large amount of steps.

$$\boldsymbol{\Delta t \leq \Delta t_{critical} = \frac{2}{\omega} = \frac{L}{C}} \text{ .... } \mathbf{4\text{-}8}$$

Where, $\omega = \sqrt{K/_{M}}$

Solid elastic stress wave speed (C) in a given material is then given by:

$$C = \sqrt{\frac{E_0}{C}}$$

Where E_0 is the initial elastic modulus (i.e. before plastic deformation) of the material and ρ is the mass density. The largest stable time step for a given material is therefore:-

$$\boldsymbol{\Delta t = L_{min}\sqrt{\rho/E}} \text{ .... } \mathbf{4\text{-}9}$$

Where, L_{min} is the smallest distance between any two nodes of the numerical crash simulation model.

Since this distance can change during a simulation, the stable time step changes and must be updated continually as the solution proceeds in time. When using steel, the typical value of the stable time step is about one microsecond when the smallest discrete node distance in the mesh of the finite element model is about 5 millimeters. It needs then about more than 100,000 time intervals to solve a crash event that lasts for one tenth of a second.

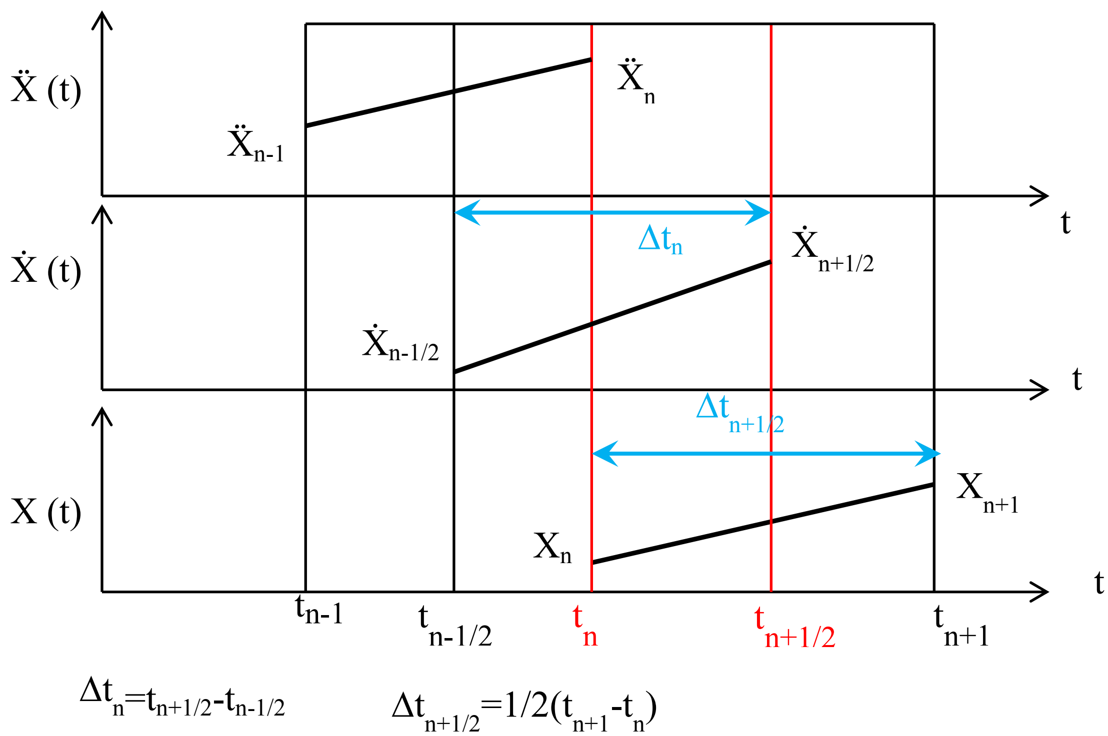

Figure 4-1 Central difference time integration methods

The velocity and displacement vectors can be calculated as

- $\dot{X}_{n+1/2}=\dot{X}_{n-1/2}+\ddot{X}_n\Delta t_n$
- $X_{n+1}=X_n+(\dot{X}_{n+1/2})(\Delta t_{n+1/2})$

The geometry is updated by adding the displacement increments to the initial geometry $\{x_o\}$:

- i.e. $X_{n+1}=X_n+(\dot{X}_{n+1/2})(\Delta t_{n+1/2})$

E.g. $X_1 = X_0 + \dot{X}_1 * \Delta t$

$X_2 = X_1 + \dot{X}_2 * \Delta t$

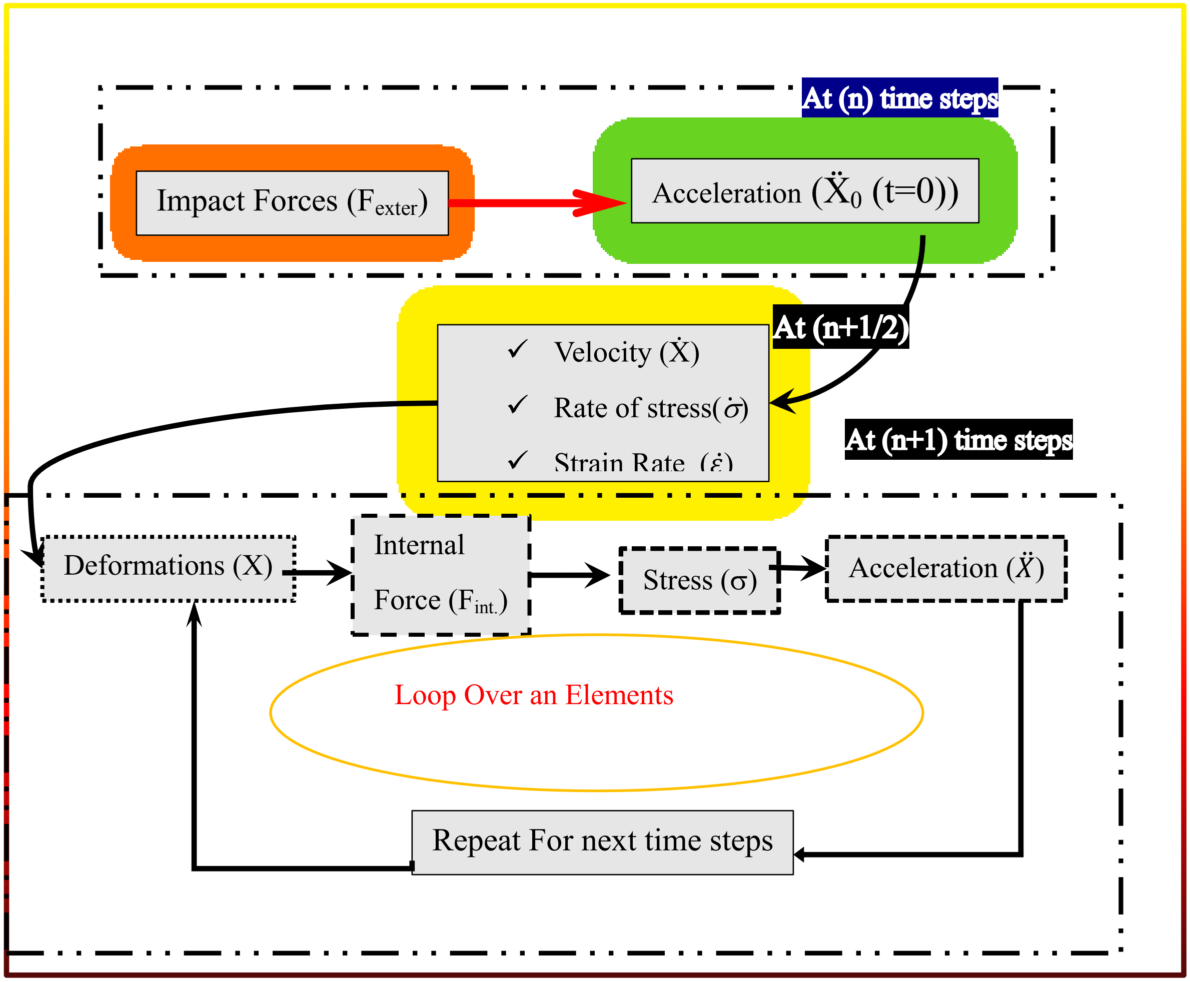

Figure 4-2 Flow charts of central difference time integration methods for time step n

4.3 Crashing Element Component Model

a. Honeycomb energy absorber simulation and test: Aluminum honeycomb structures are characterized by high weight/strength ratios, high energy absorption capacity, long stroke, stable deformation on out-of-plane direction and low weight. Because of these characteristics, honeycombs structures are widely used in airplane, automotive industry and railway vehicles in order to improve the crashworthiness of vehicles. Crashworthiness parameters of Aluminum honeycomb structures depend on the cell specifications such as expanding angel, foil thickness, length/thickness ratio and impacting velocity. These structures are produced by manufacturers in different cell sizes and specifications. In order to select the structure with high crashworthiness parameters, it is required to test experimentally and numerically.

E_{abs}≈Crushing Force*Stroke,

$$\mathbf{E_{abs.} = F_{crush} * L_{C}} \qquad 4\text{-}10$$

Where, $\mathbf{F_{Crush} = \sigma_{crush} * A_{crush}}$, $\mathbf{L_C}$, crush distance

b. Primary energy absorber simulation: The primary energy absorption tubes are the key component of crush zone system. In order to design the thin-walled tube with high crashworthiness performance, a comparative study on the crashworthiness parameters of tubes having circular, square, ellipse cross-section, pyramidal and conical shapes have to be evaluated for comparison. In the light of finite element simulation results and theoretical studies, it is found that pyramidal tube has the highest crashworthiness parameters with a stable crush behavior.

The requirement for absorbing impact energy of the rail vehicle, to improve crash worthiness, the material could be properly selected .The energy absorbed during collision can be approximated as the product of the mean crush load and crushing distance(6).

The energy absorbed can be calculated as:

$$\mathbf{E_{abs} = \sigma_{crush} * A_{upp} * D_{upp} * 0.8} \qquad \mathbf{4\text{-}11}$$

Where, E_{abs} =energy absorbed, F_{ml}=mean crushing load, S_{crush}=crushing distance

δ_{crush} =crushing stress, A_{upp}=is the area of upper absorber, D_{upp}=Depth of the absorber, 0.8=assumption for absorber stroke. Rearranging the above equation gives

$$\sigma\text{crush} = \frac{\text{Eabs}}{\text{Aupp} * \text{Dupp} * 0.8}$$

Thus, by varying the crush load, absorbed energy will vary and this makes to select material which meets energy absorption standard requirements.

The proof stress (δ_{proof}) for the absorber can be determined from the proof load (F_{proof}) and load area (A_{load}).

$$\boldsymbol{\sigma}\text{proof} = \frac{(\text{Fproof})}{(\text{Aload}).}$$

Using the design developed for finite element model; under dynamic analysis it is quite simple to understand its energy absorption capabilities during impact load.

4.4 Approaches for Improving Crashworthiness

Many studies have considered for crashworthiness enhancement of vehicle structures by selecting optimal properties of material and geometry (thickness/cross-section) for major load carrying members or by introducing additional load paths to the structure.

The concept of improving the rail vehicle cab structure for crash worthiness has been developed significantly over the last few decades having a variety of reliable modeling tools. Researchers have used these modeling tools to analyze and improve vehicle designs for this safety conditions. The approaches for improving crash worthiness are geometry and material improvements:

4.4.1 Geometry Optimization (Enhancement of stiffness)

As for realizing crashing elements there are more operational principles for absorbing impact energy.

1. Dry friction shock absorber

Dry friction shock absorber is the impact energy damping principle where a piston moves in a cylinder against a high friction forces caused by special normal force generating elements.

2. Honeycomb

Honeycomb impact energy damping capacity is based on plastic deformation principle of the material.

3. Thin walled tubes

This is also by plastic deformation principle, where the structural profile is plastically deformed under impact energy. In this paper thin walled cylindrical, rectangular, square, hexagonal and octagonal tube profiles have been investigated as a candidate for crashing element model selection for their simplicity. The material selected for this five mentioned profiles Table 4-1 is commonly used steel that can be used for crash worthiness structure. Over the length of the longitudinal member, the profile thickness kept constant at 6.0 mm. This value is realistic and generally gives a stable deformation patterns. The dimensions of the profiles have been chosen to have the same perimeter resulting in a constant mass per unit of length. The original non deformed length of each profile is 350 mm.

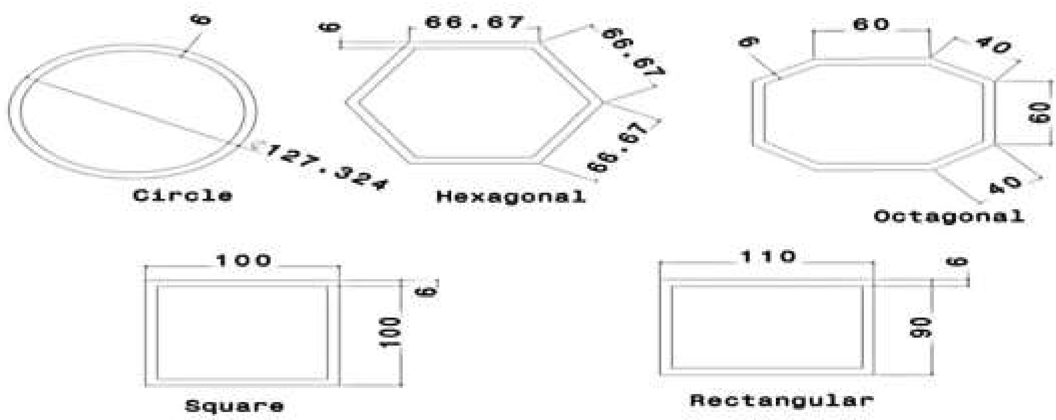

Figure 4-3 Crash Component Geometry Modeling

Table 4-1 Dimensions for selected five different geometries with the same perimetre per unit length and mass

profile	Shape	Perimeter(mm)	Area(mm^2)
A	square	4*100=400	100*100=10000
B	Rectangular	2*(110+90)=400	b*h=110*90=9900
C	circle	π*d=π*127.324=400	π*r^2=π*63.662^2=12732.405
D	hexagonal	6*s=6*66.67=400	296340.743
E	octagonal	4*(60+40)=400	5760000

The results of geometry performance simulations by Baaten 1994, which concerns the collision with a 56 km/h impact speed, a mass of 1100 kg, and a normal angle of incidence, are shown in figure 14. Both extremities of the column have non deformable plate (rigid body), this is more realistic (normally they have a connection with stiffer vehicle components) and better for mutual comparison and to exclude different end effects. The energy absorption is plotted as function of its deformation length (rather than a function of time) because this facilitates the comparison of different structural crash analysis concepts.

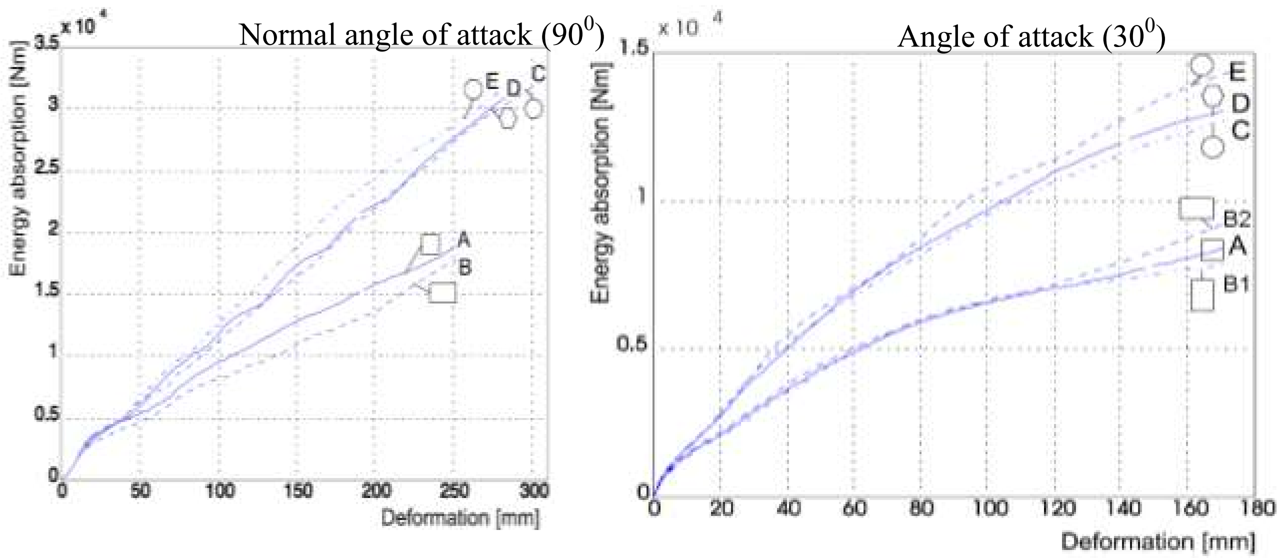

Figure 4-4.Energy Absorption of different geometries with a load direction of 0^0 and 90^0 (12)(non-Linear)

For the second graph, it has the same collision impact velocity of 56 km/h and a vehicle mass of 1100 kg but here with an angle of incidence of 30 degrees. With an oblique load direction, numerical simulations of the cross-section of the rectangular profile are carried out in two orientations: standing (profile code B1) and lying (profile code B2). It can be expected that in lying position the higher bending resistance of the profile results in a better energy absorption.

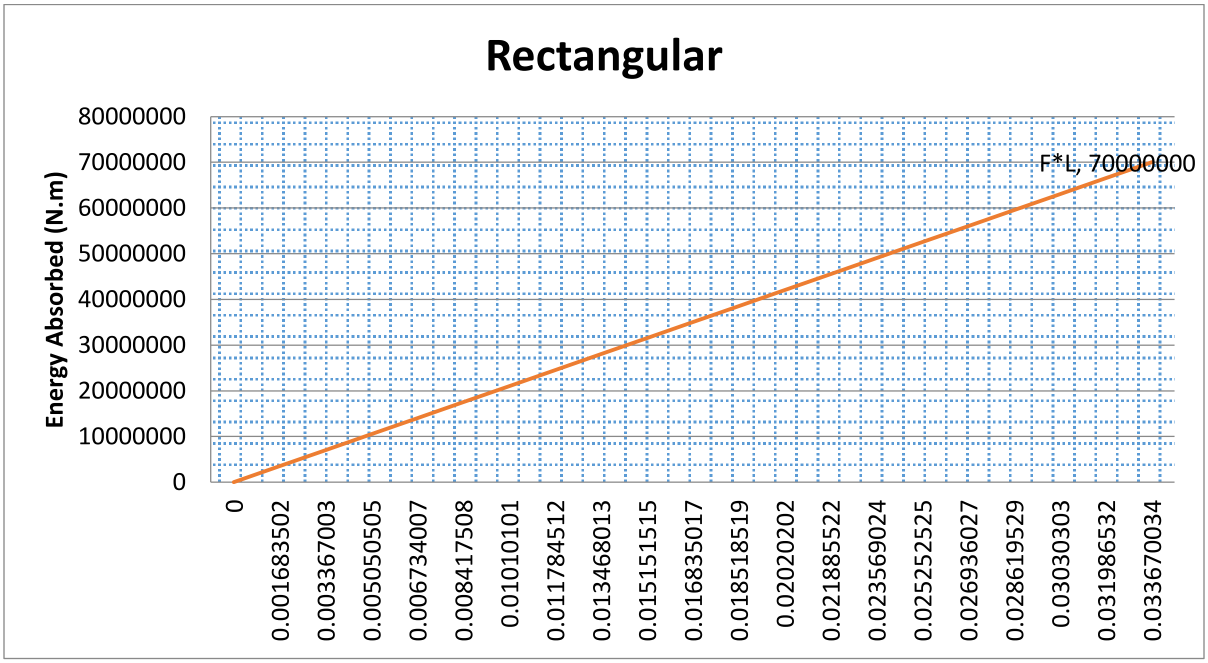

Figure 4-5 Energy vs. Deformation graph for Rectangular profile

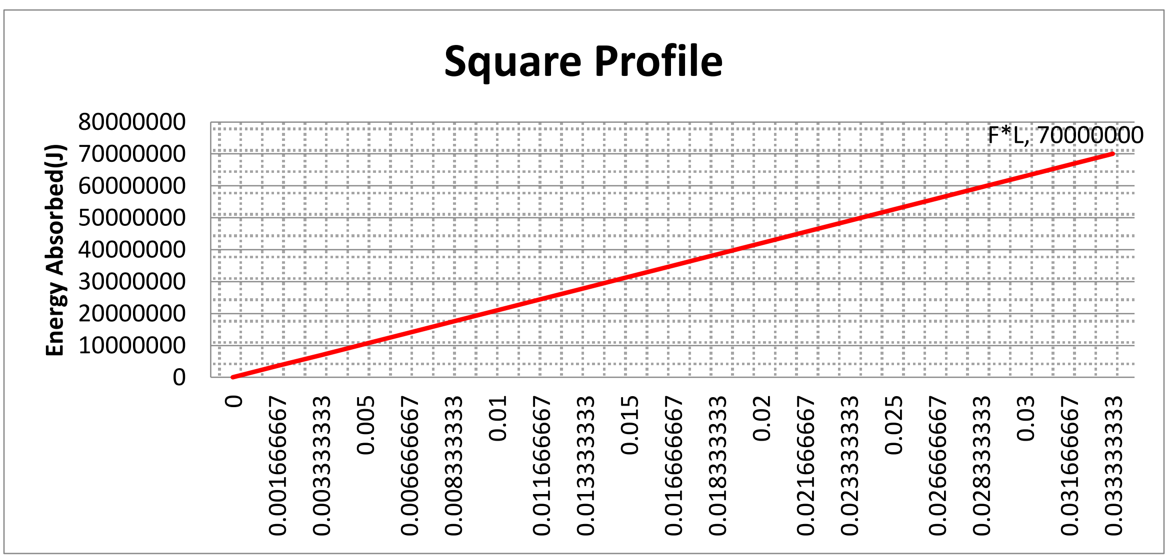

Figure 4-6 Linear Energy absorption capacities of square profile

The energy absorption capacity for square profile for linear estimation, i.e. roughly to select the geometry of impact energy absorber profile, indicates that to absorb 700KN.m impact energy the deformation is about 0.33m.which is less than rectangular profile deformation.

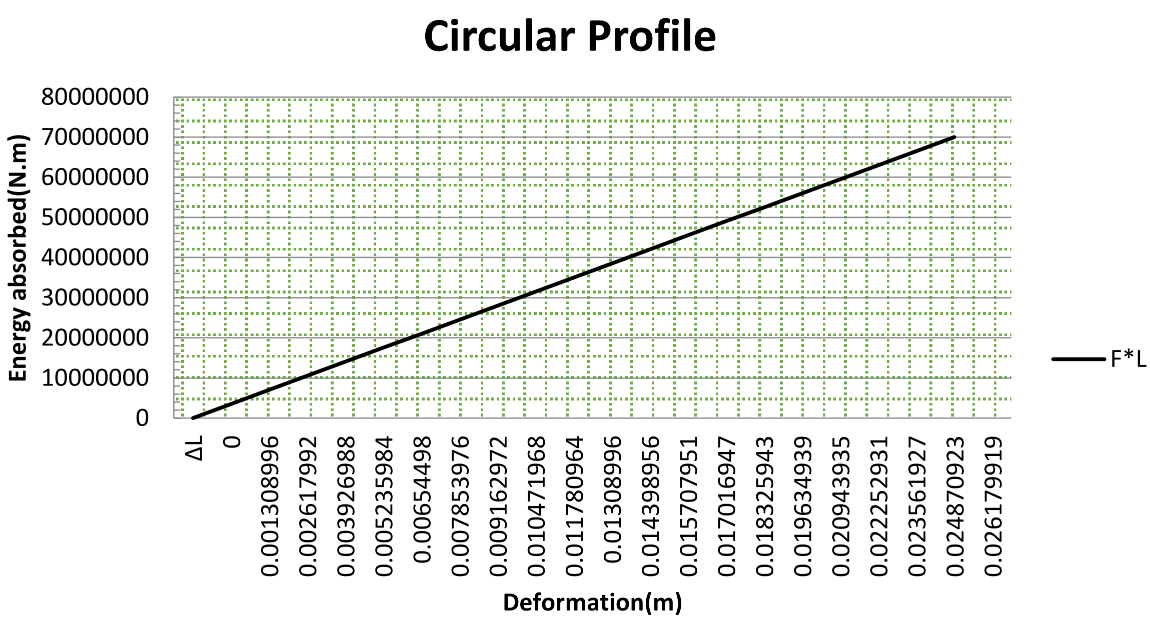

Figure 4-7 Energy vs. Deformation graph for Circular profile

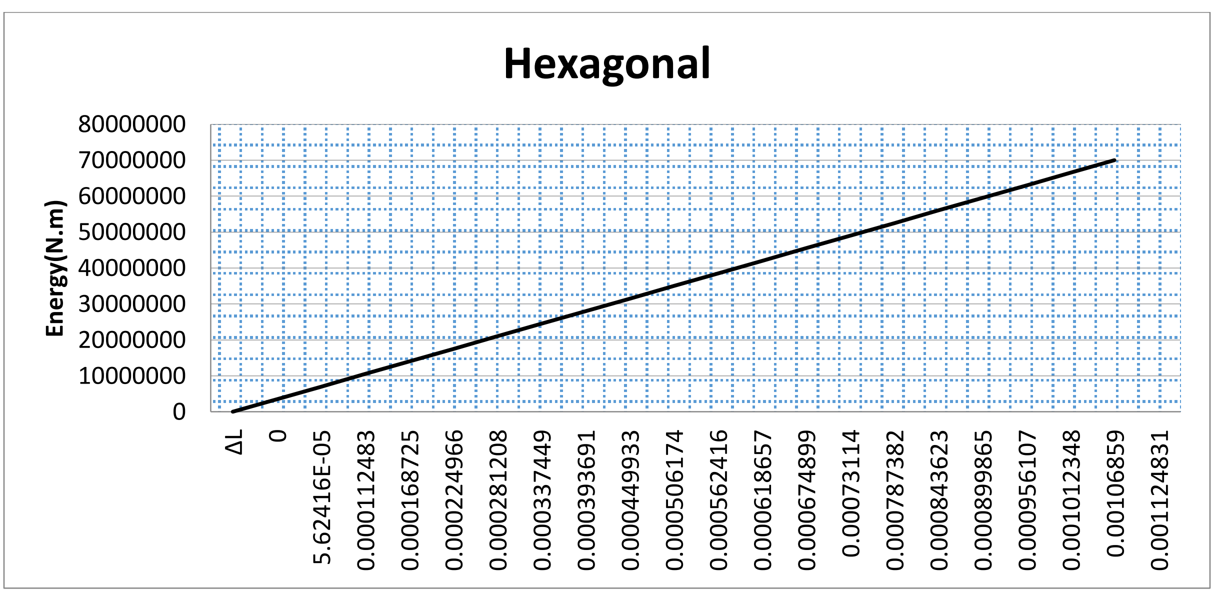

Figure 4-8 Energy vs. Deformation graph for Hexagonal profile

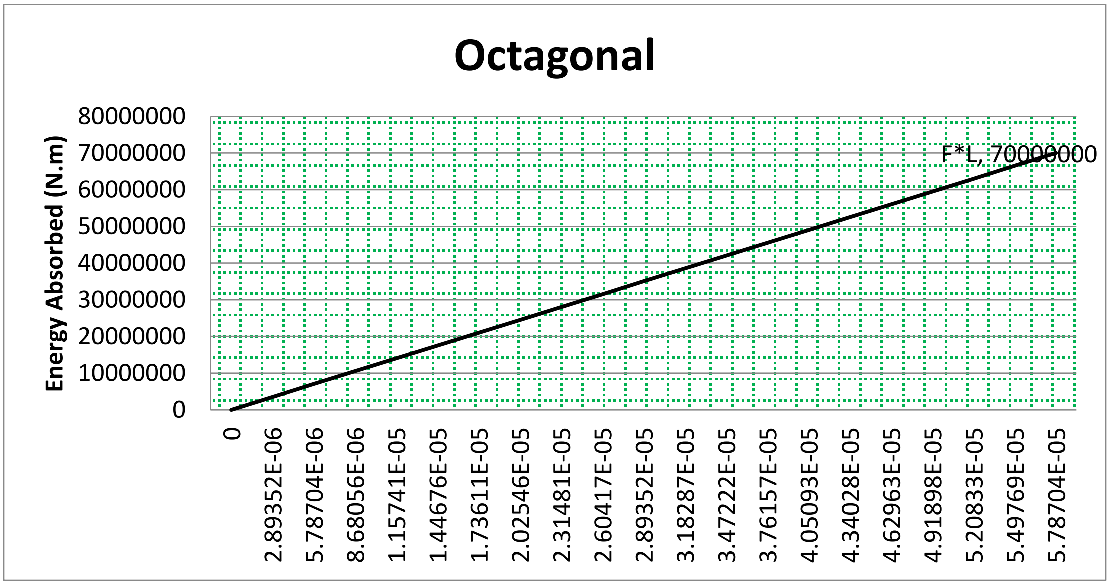

Figure 4-9 Energy vs. Deformation graph for Octagonal profile (Linear)

Based on these analyses, it can be concluded that a square and a rectangular profile have significantly lower energy absorption than the other three profiles. The octagonal profile absorbs slightly more energy during its deformation than the circular and the hexagonal profiles, which absorb nearly the same amount of energy. The circular profile yields the longest possible deformation length and, hence, is capable of absorbing slightly more energy in its final deformation.

4.4.2 Material Selection for the Structure

Material's role is one of the most needs considerations in crashworthiness enhancement. Lighter materials are being developed to reduce vehicle's weight, cost and running energy consumption. At the same time these lighter materials should maintain the safety of the vehicle stiffness desires according to the standard requirements. Significant research work has been conducted to achieve these objectives.

- ❖ Material Modeling for selection of crush worthiness application is based on
- ✓ the **effect of Strain Rate** and
- ✓ **effect of Heat (thermal) (Conductivity)**

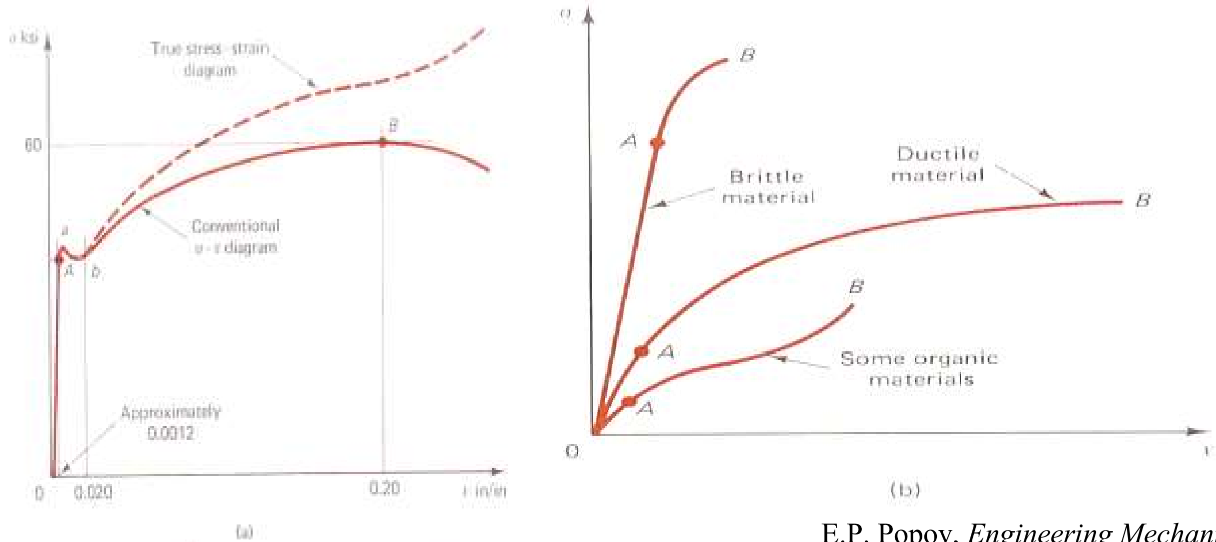

E.P. Popov, *Engineering Mechanics of Solids*. New Jersey: Prentice Hall, 1990.

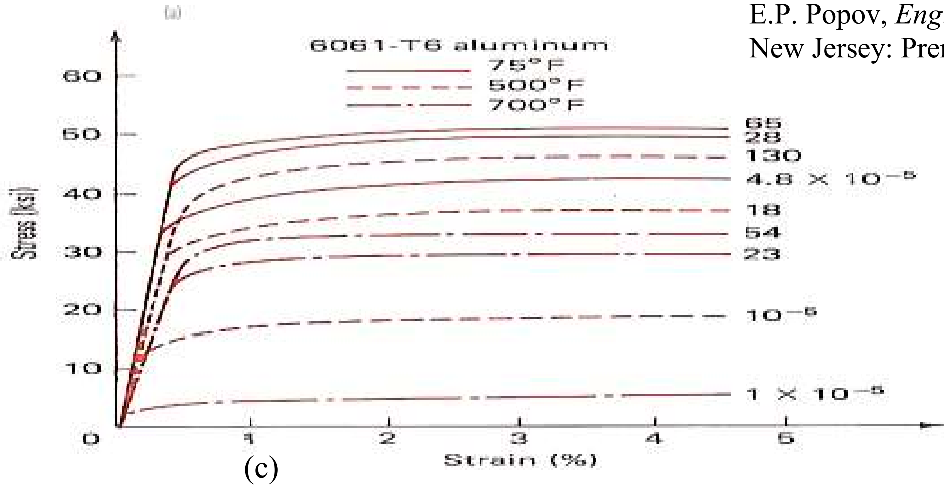

Figure 4-10 Stress strain diagram (a)Mild steel and (b)Typical Material, Effect of Strain Rate and Temperature (c) for 6061-T6 Aluminum Alloy (15)

As we can see from stress-strain rate graph when the temperature rise due to collision frictional force the stress reduces while the strain rate rise rapidly and the structural deformation considerably increases.

a. Steel

Steel sheets have been used in vehicle structures for more than one century. Its low production costs, consistent properties and the huge accumulated and available knowledge about its production processes make it the material of choice for rail vehicle manufacturers. Its crashworthiness performance has been studied by several researchers. Van Slycken et al. (16)

studied high strength steels potentials for crashworthiness. They showed that high strength steels under dynamic loading experience higher energy absorption capacities and these capacities even increase as the strain rate increases, which is an advantage for crash energy absorption applications. Peixinho et al. (17) examined the crashworthiness behavior of thin walled tubes made of dual phase and transformation induced plasticity (TRIP) steels. TRIP steels are steels containing a metastable austenite that transforms into martensite during plastic deformation, which allows for enhanced strength and ductility (18). They conducted tensile tests at different strain rates as well as axial crushing tests. Their test results showed that TRIP steels are **strain rate sensitive** and this can be useful for crashworthiness applications. They used LS-DYNA to model the tests, and numerical and experimental results were in good agreement. Hosseinipour et al. (19) studied improving the crash behavior of steel tubes by incorporating annular grooves. They showed that this may lead to a controllable progressive deformation, thus increasing the energy absorption capacity of the tubes.

4.4.3 Material Models Considering Strain Rate effect

The influence for material selection for impact energy absorbing conditions is mainly depends on the structure compression velocity. In case push-through deformation processes it is enough to consider the dependence of the energy amortization on the impact velocity.

- Strain rate independent material Model

The energy absorbed by a given type of crash element doesn't depend on the compression velocity within the computational accuracy of 10%.

- Strain-rate dependent material Model

When the strain rate effect has to be taken into consideration, then the following relation can be used as (3).

$$(\boldsymbol{\delta})^{din} = \boldsymbol{\delta}^{Stat}(\boldsymbol{\varepsilon}_{Plastic}) + \boldsymbol{R}_{eH}\left(\frac{\dot{\varepsilon}}{C_M}\right)^{\frac{1}{P_M}} \qquad \textbf{4-12}$$

Where σ^{din}=dynamic stress, σ^{Stat}=Static stress, $\varepsilon_{plastic}$=plastic strain, $\dot{\varepsilon}$=Rate of plastic strain, R_{eH}, and constants P_M, and C_M are to be specified by means of material test.

For the compression velocity dependence of the absorber energy on the basis of several numerical tests in case of push-through deformation the following quasi-numerical formula can be evaluated by numerical regression analysis.

$$\boldsymbol{E(V) = E(0)\left(1 + \frac{V}{C_E}\right)^{\frac{1}{P_E}}} \quad \textbf{4-13}$$

Where, PE≈P_M and this two equations are very essential as energy absorption capacity can be estimated for a specific compression velocity without many simulation requirements. Due to the strain rate effect the influence of the selection for the material model for the impact energy absorption, it is required from the point of view of the compression velocity. In case of push-through deformation process it is enough to consider the dependency of the energy amortization on the impact velocity

CHAPTER-5

5 RESULTS AND DISCUSSION

5.1 Simulation for Collision Dynamics

The initial step of finite element method (FEM) analysis is a time domain simulation of the frontal train cab for Light rail transit (LRT) under collision. Based on the time dependent force function FEM based structural dynamic computations can be carried out to determine the time dependent elastic/plastic deformation process. As a result of FEM computations second approximations of the plastic deformation dependent inter -vehicle force transfer conditions can be evaluated in the form of force transfer conditions and it can be then evaluated for non-linear connection force versus plastic law.

There are several ways to classify the rail vehicle accidents due to collision. A possible classification is to make distinction between longitudinal and side impacts. Generally, this can be grouped under three main categories.

a. Train to train collisions
b. Train collision with high way vehicles at level crossing
c. Train collision with obstacle due to derailment.

The Cab model has the total length of about 4.25m total length, 2.5m width and 3.4m height (all measured values are external). It consists of frontal structures that damps impact energy for which it is required that majority of impact is frontal collision. The model has been done using CATIA V5 R19 software as shown in Fig. 5-1. The structure has multiple structural components but the main crashing are Cab nose, Main energy absorber, upper and lower energy absorber, anti-climber, roof energy absorber, Cab shell and supporting pillars and honey comp plate (or pillars connecting plate).

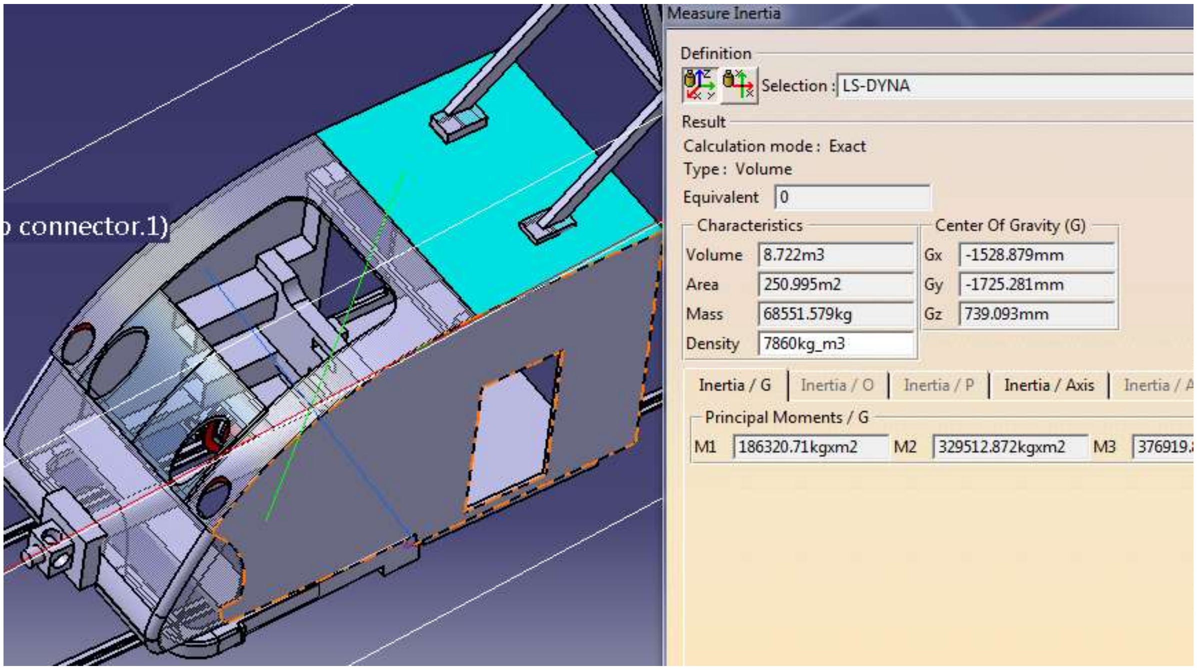

Figure 5-1 Over all Dimensions of the Model

Each and every detail part is modeled in separate part and then assembled using CATIA assembly work bench using assembly constraints. Then the model is exported to the ANSYS LS-DYNA to mesh and test the model under collision dynamics.

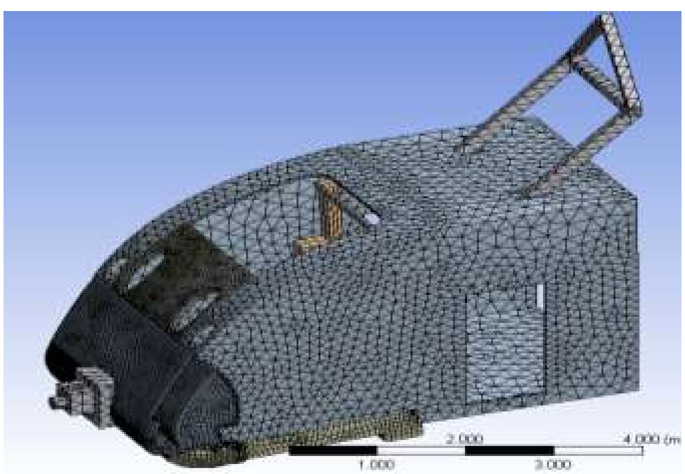

(a)

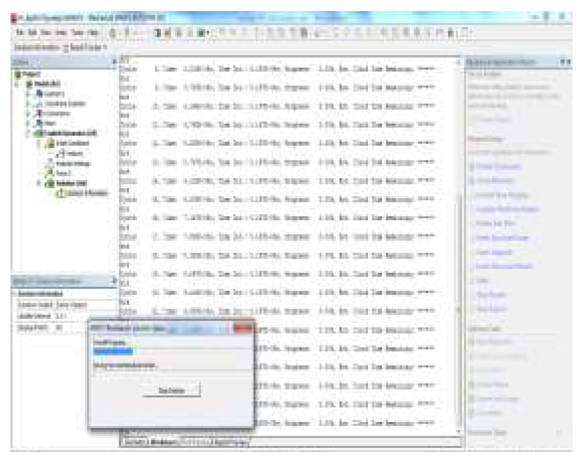

(b)

Figure 5-2 ANSYS (LS-DYNA) (a) Finite Element Meshing (b) Explicit/ Analysis solution stages

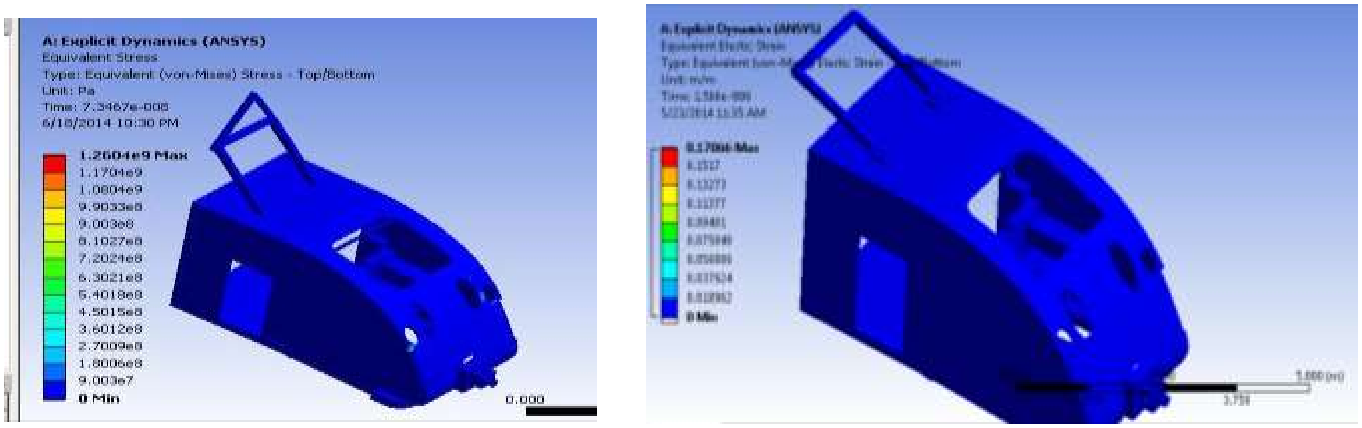

(a) (b)

Figure 5-3 Equivalent Von-Miss stress (a), Elastic Strain (b)

It can be seen that the equivalent Von-Miss stress under 100KN impact load, is 1.1704GJ.

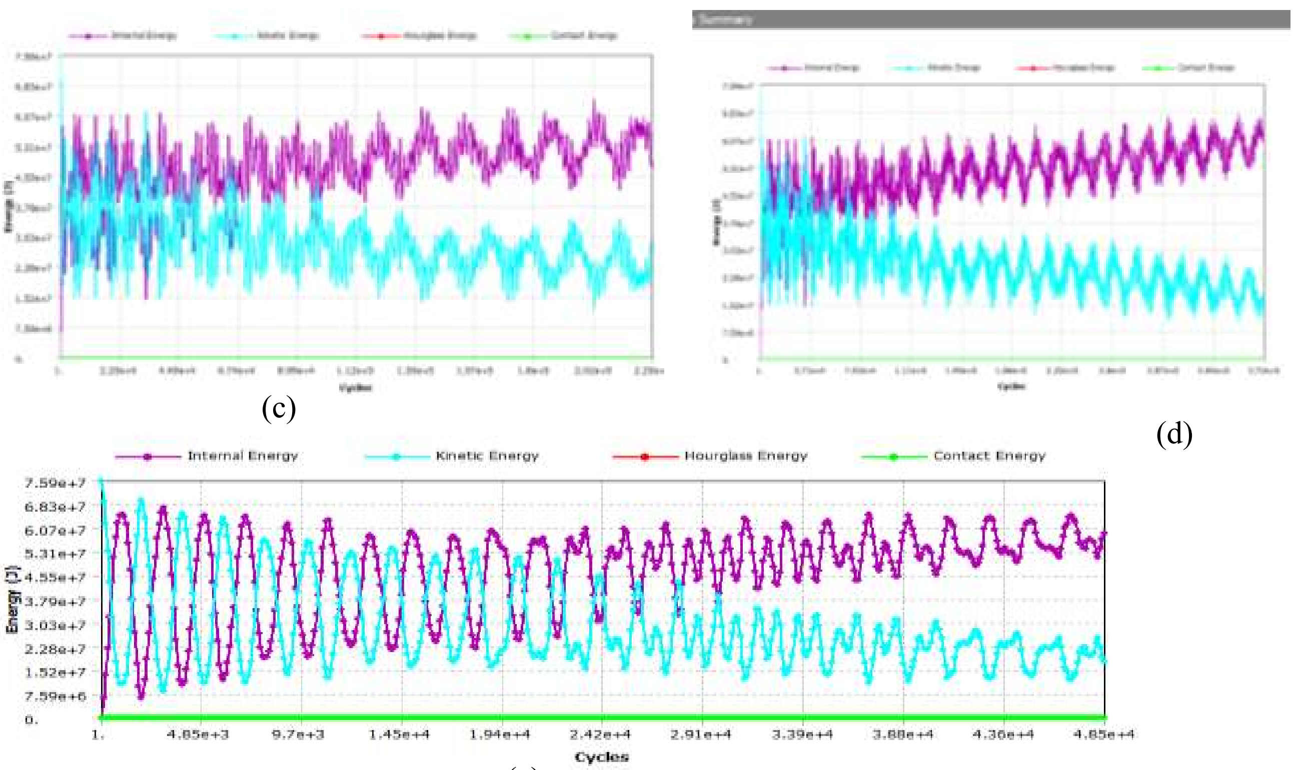

(c) (d)

(e)

Figure 5-4 (c)Kinetic Energy and Internal during Collision Simulation at time t1(d) Kinetic Energy and Internal during Collision Simulation at time t2(e) Kinetic and Internal Energy vs. Cycles duration

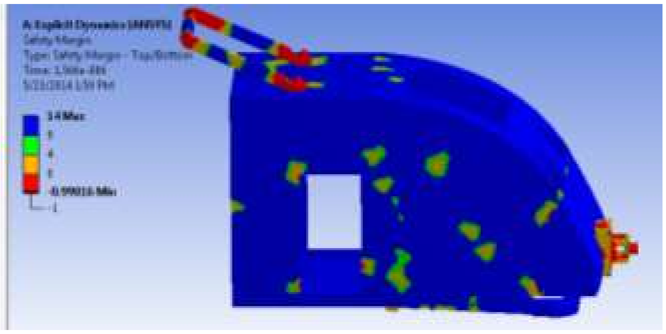

(f)

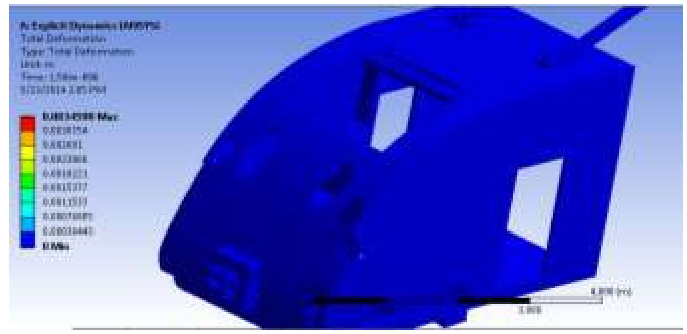

(g)

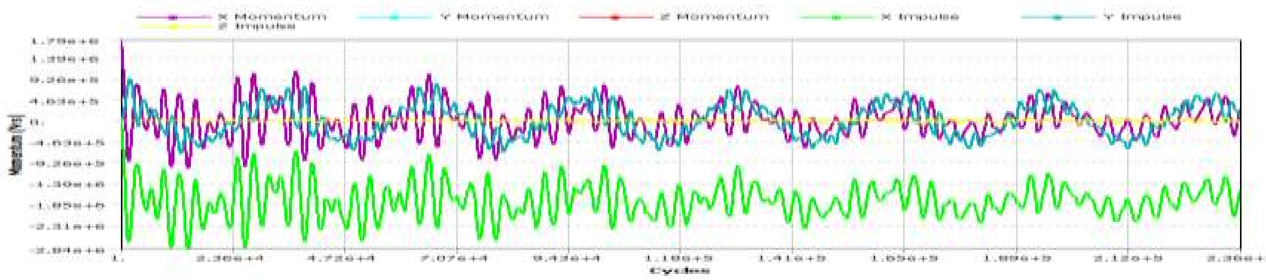

(h)

Figure 5-5 Safety Margin Simulation results (f) and Total Deformation (g), (h) X-momentum and X-impulse graph

5.2 Simulation for Impact Energy Absorbing Elements

a. Honeycomb and Supporting Pillars

Supporting pillars are characterized by high weight/strength (i.e. stiffer) ratios, high energy absorption capacity, long stroke, stable deformation on out-of-plane direction and low weight. Because of these characteristics, honeycombs structures are widely used in airplane, automotive industry and railway cars in order to increase the crashworthiness of vehicles. Crashworthiness parameters of Aluminum honeycomb structures depend on the cell specifications such as expanding angel, foil thickness, length/thickness ratio and impacting velocity. These structures are produced by manufacturers in different cell sizes and specifications (13). In order to select the structure with high crashworthiness parameters, Numerical simulation have been conducted for a specific compressive capacity under impact load. In the honeycomb box, 2 aluminum honeycomb blocks with 30×25×2500mm dimension are positioned. These blocks absorb about 0.1288245MJ energy in 6.44cm stroke.

Total Energy Absorbed=Crushing force*Deformation (Stroke)

$E_T=P_{Crush.}*L_{stroke}$... 5-1

Where, $P_{Crush} = \sigma_{Strock} * A$, Let impact force P=2000KN, E=207Gpa

$$E = \frac{\sigma}{\varepsilon} = \frac{PL}{A\Delta L}$$

- $\Delta L = \frac{PL}{AE}$

$A=0.03*0.025=0.00075m^2$

E, Young's Modulus of Elasticity=207GPa

$\Delta L=2000000*0.5/(0.00075*207*10^9)$

=0.0644m

ΔL =6.44cm

E_T=2000000*0.0644

E_T=0.1288245MJ

$\sigma_{Crush}=P_{Crush}/A$,

Where, A is the *perpendicular area under impact force* **=1.735*0.25**

$A=0.43375m^2$

σ_{Crush}=0.5*2000000/0.43375 (two pillars)

σ_{Crush}=2.3055MPa

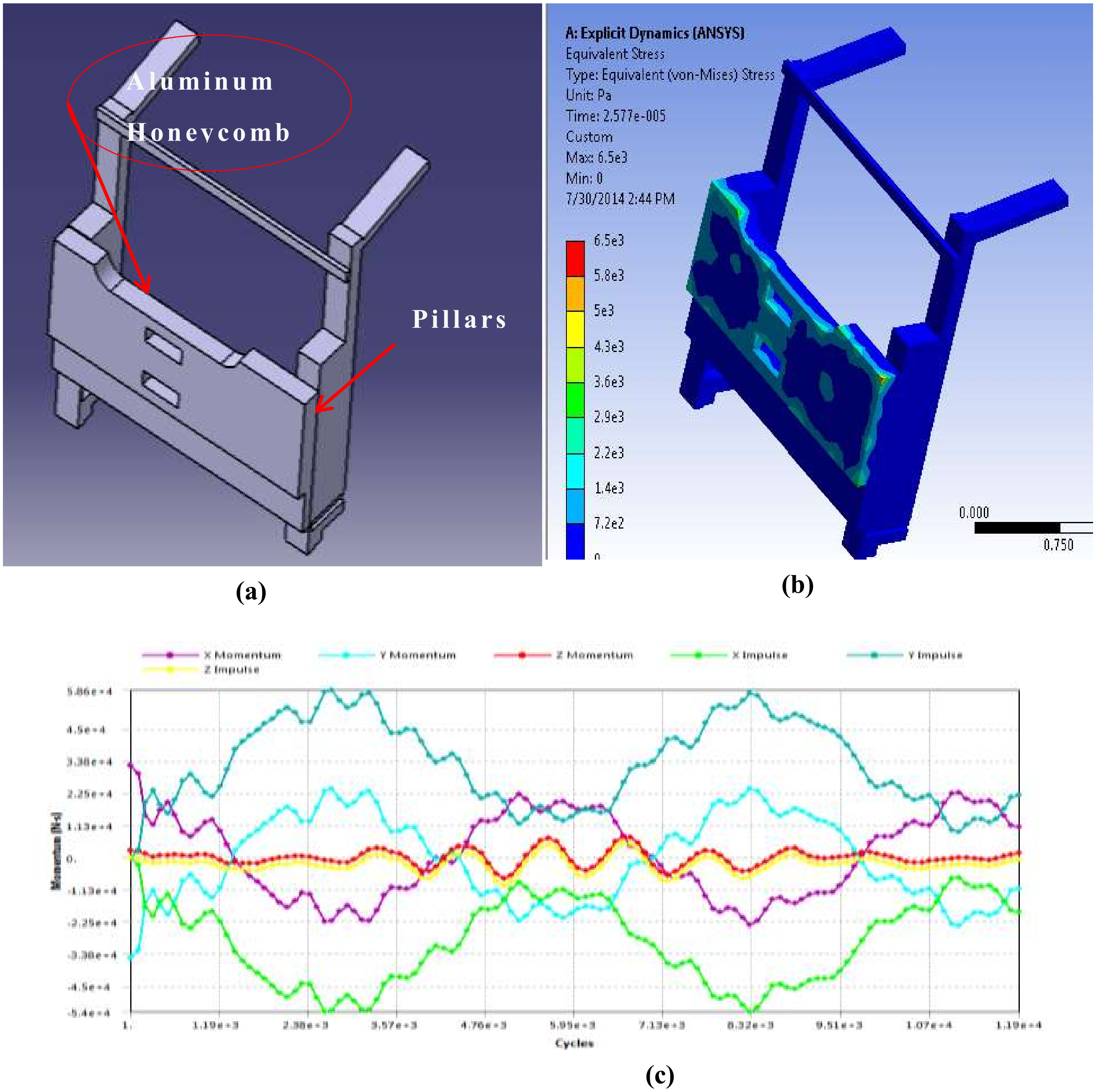

Figure 5-6 Supporting pillars and Honeycomb structure (a) 3D Model (b)Simulation Results (c) Momentum vs. duration at a specific cycle intervals

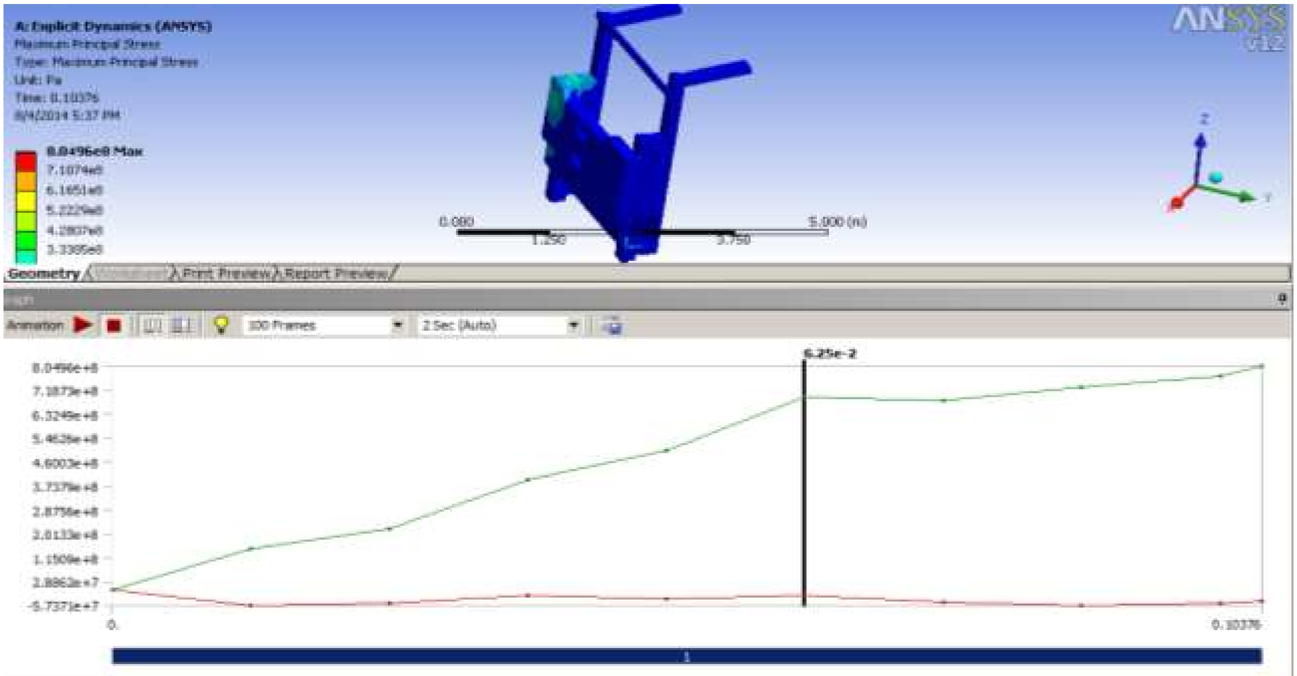

Figure 5-7 Maximum Principal Stress vs. Impact Durations

The material chosen to meet this requirement could be determined from the material selection tables provided by Hexcel Company for their 5052 Aluminum Alloy Hexagonal honeycomb. The suitable materials are 1/8-5052- 6.1 with 3.1MPa crushing stress and 1/4-5052-6.0 with 3.0MPa crushing stress. In order to study the crushing behavior of the honeycomb, specimen with 30 mm width, 30 mm length and 20 mm height are modeled by using CATIA V5 R19.

In order to verify the numerical results for collision dynamic tests, material properties have to be identified. In FEM simulations for honeycomb block models, the honeycomb orthotropic (28) material model is used. Total 12 material parameters are required to model the honeycomb as follows: the Young's modulus in 3 directions, shear modulus in 3 direction and yield stress as a function of strain in 6 directions.

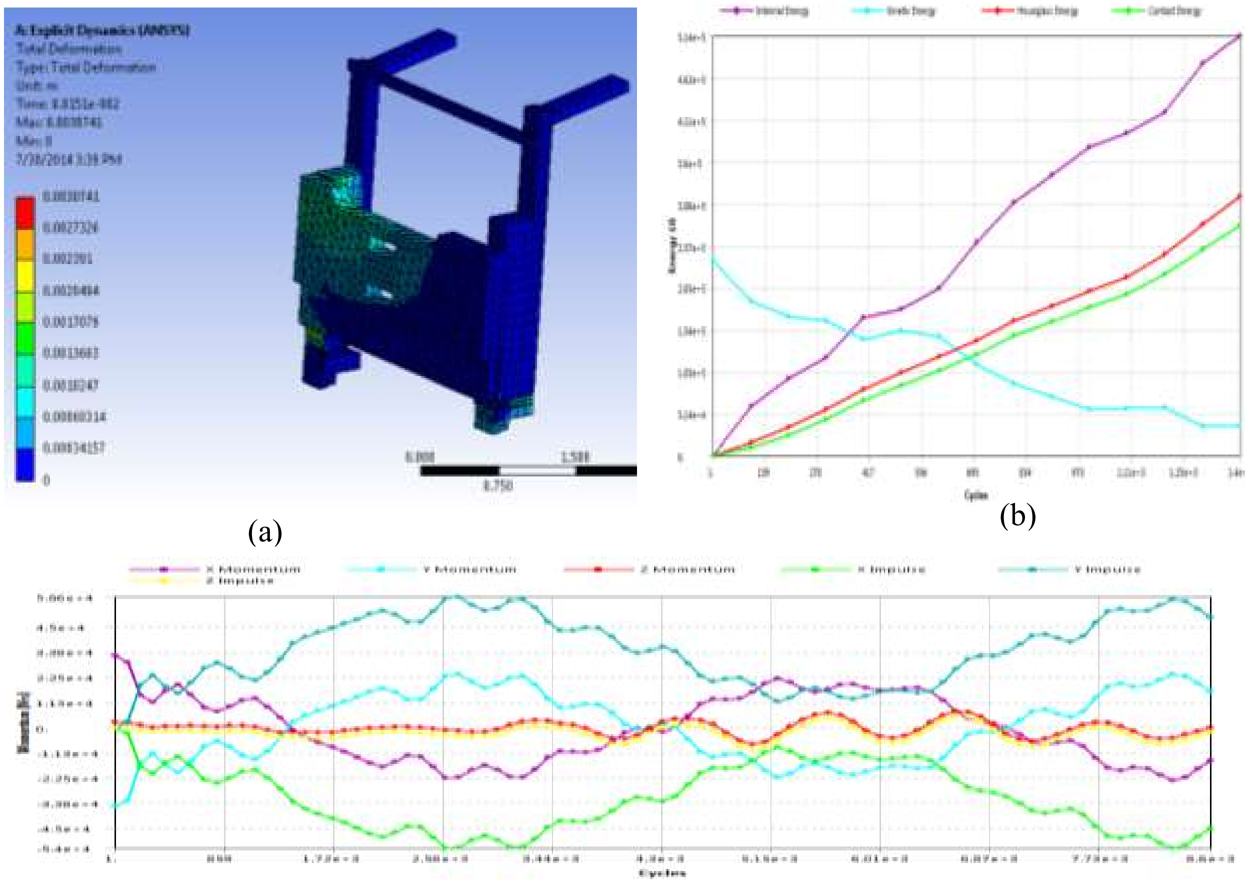

(a) (b)

(c)

Figure 5-8 Total Deformation (a), internal and KE energy (b) Momentum (c) for Supporting Pillars and Honeycomb

b. Main Energy Absorber Tubes

The tubes have the lengths of 1500mm, 750mm diameter while the thickness is 18 mm. Material properties assigned to the model are those of the mild steel A572- 50. The steel has a yield strength of =304MPa, Young's modulus of E=207GPa and Poisson ratio of 0.3.

For simulation of the dynamic axial crushing, the fixed plate is constrained in all degrees of freedom. The support plate is tied to the end of the tube, and the 2000KN crushing force is applied at one end of the tube. The tube is impacted to the fixed plate with 10 m/s downward initial velocity.

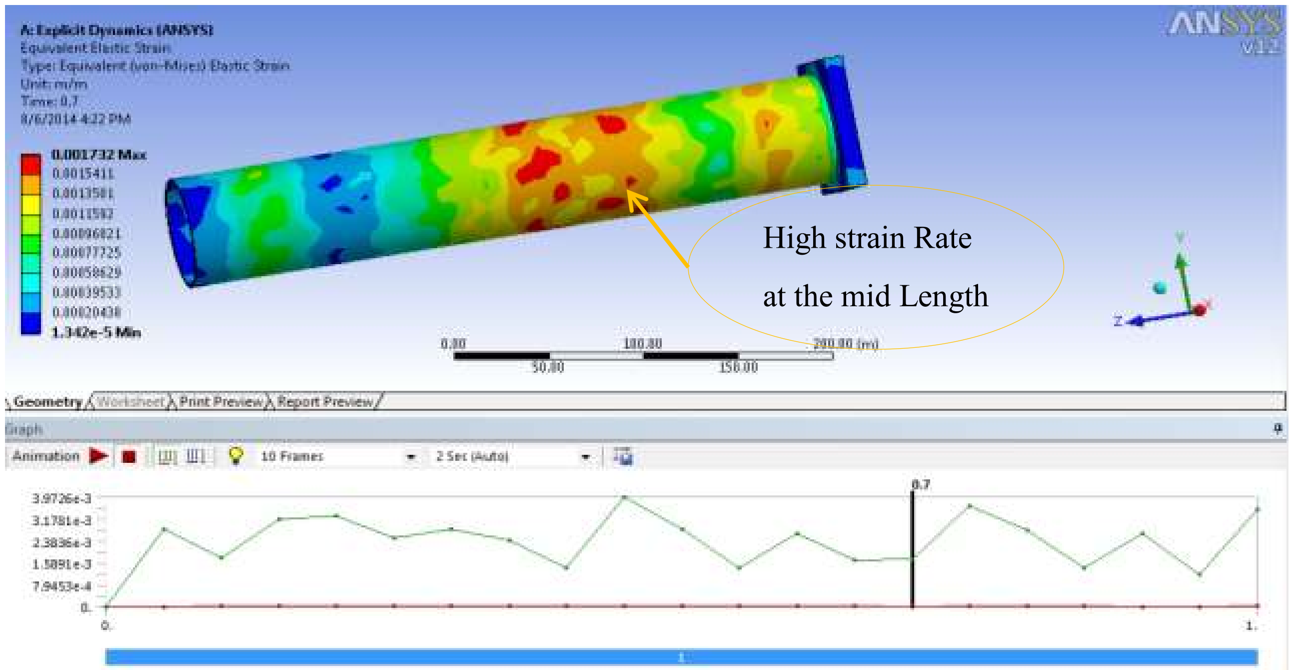

Figure 5-9 Main Energy Absorber Tube Equivalent Elastic Strain Simulation Result

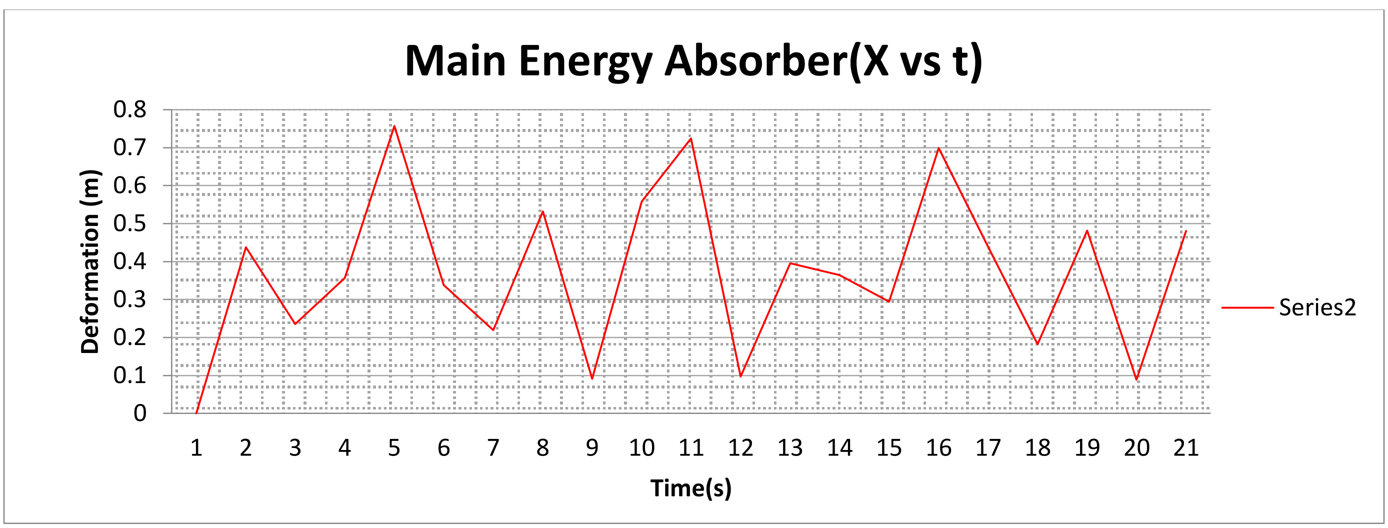

Figure 5-10 Deformation vs. time graph for main energy Absorber

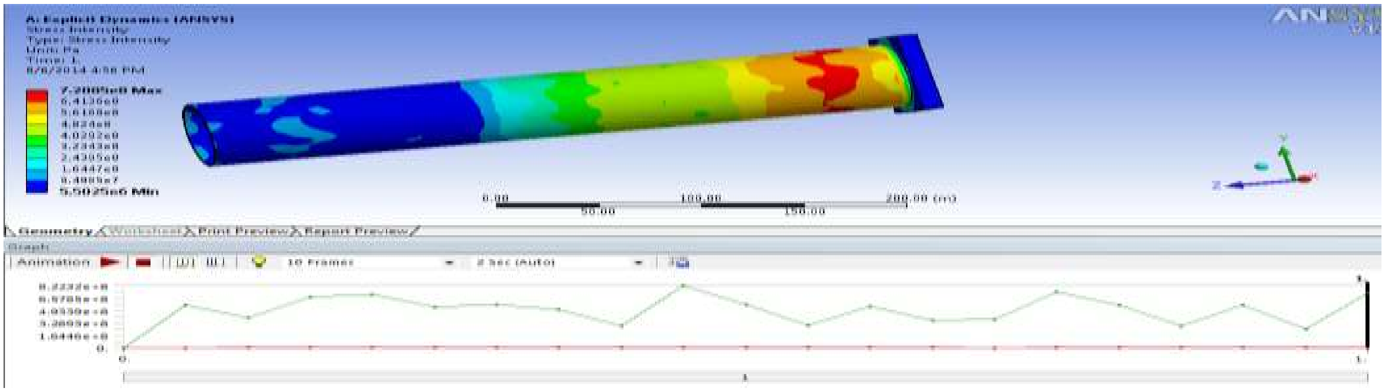

(a)

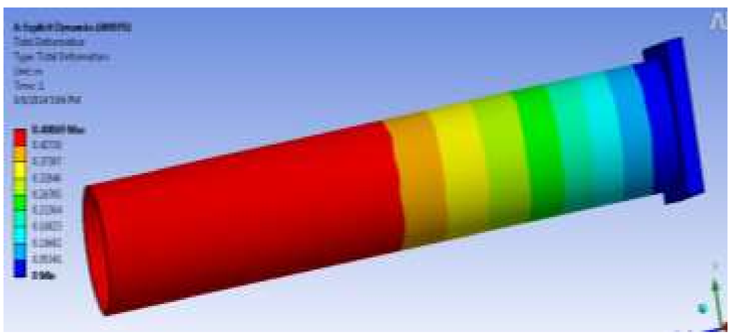

(b)

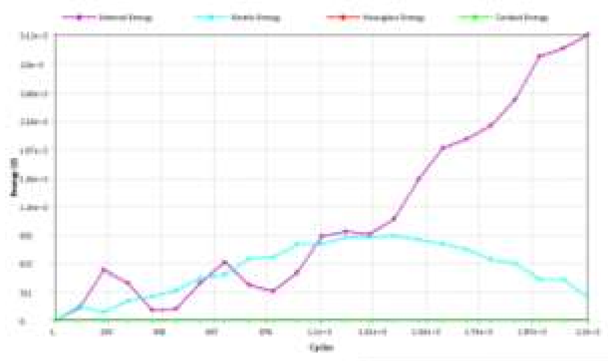

(c)

Figure 5-11 Primary Energy Absorber (a) stress intensity (b) Total Deformation (c)Kinetic Energy and Internal Energy

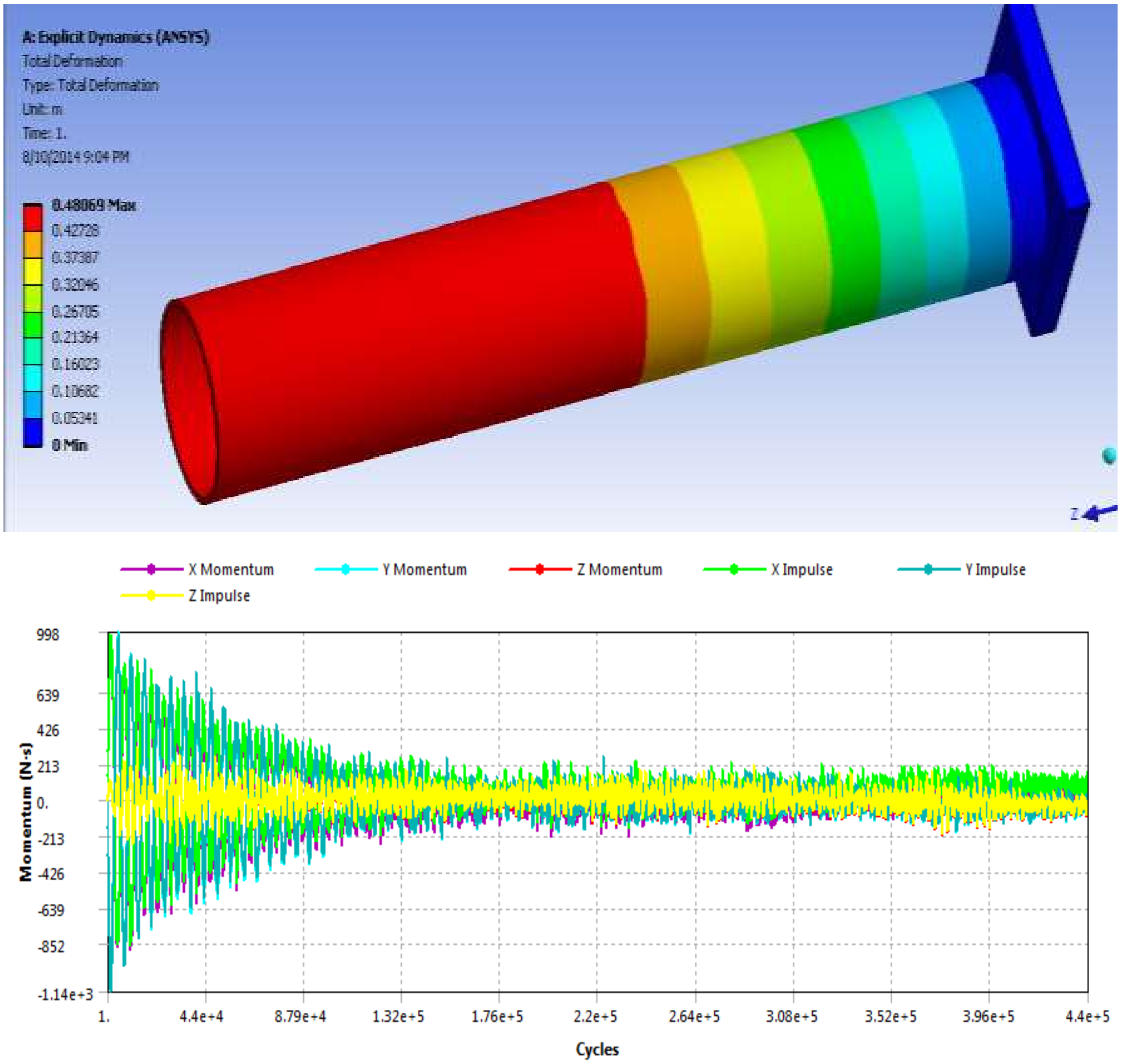

Figure 5-12 Deformation Simulation output for Main Energy Absorber profile

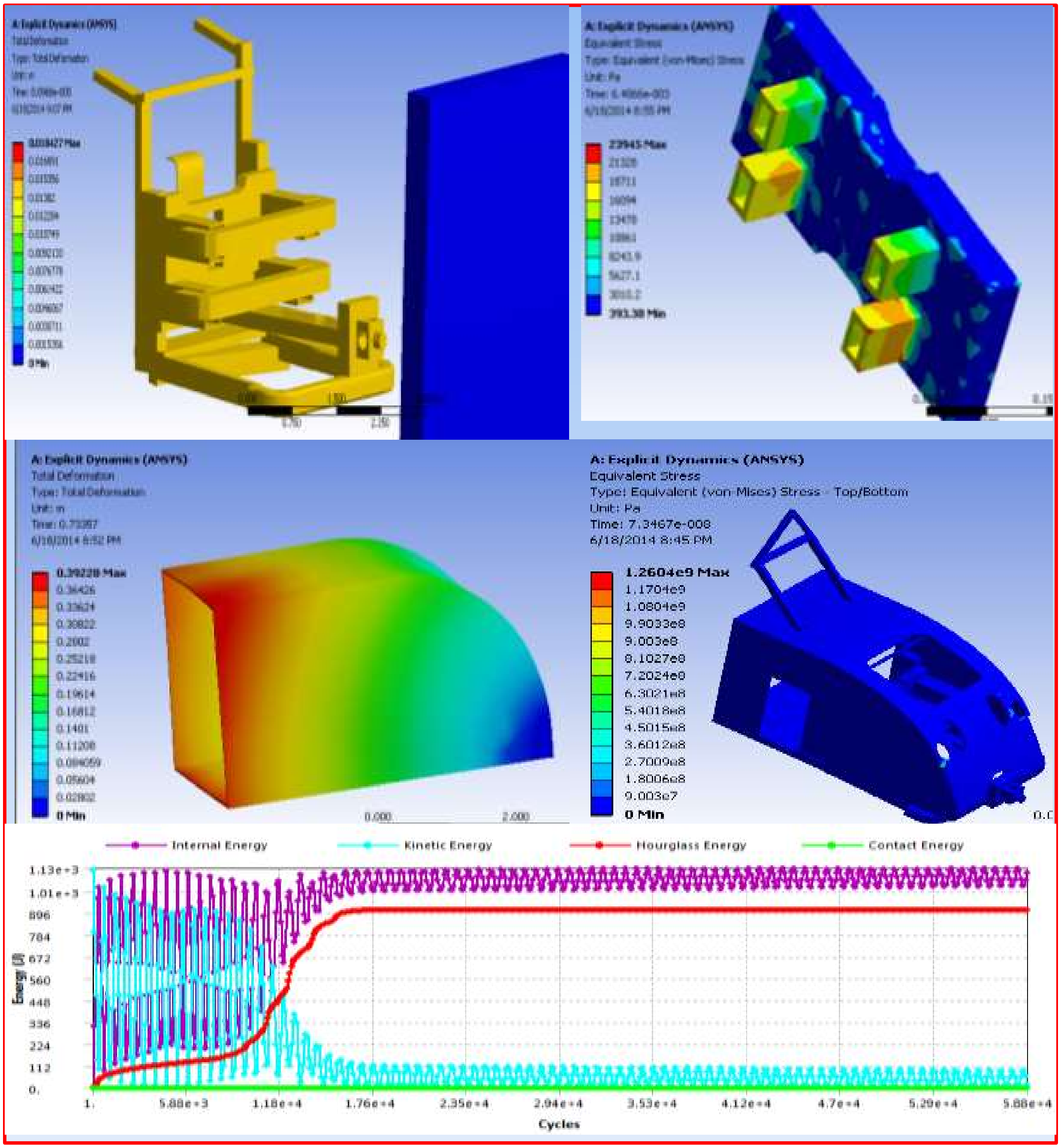

Figure 5-13 Collision Dynamics Simulation Results for variable frontal structures

.

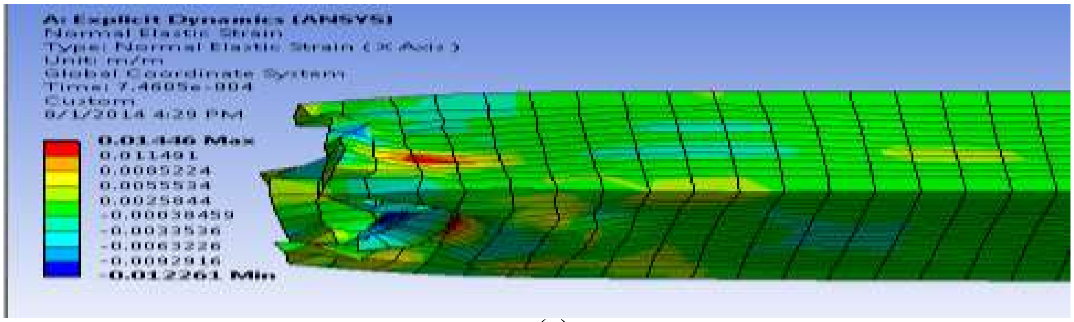
A: Explicit Dynamics (ANSYS)
Normal Elastic Strain
Type: Normal Elastic Strain (X Axis)
Unit: m/m
Global Coordinate System
Time: 7.4605e-004
Custom
8/1/2014 4:29 PM
0.01446 Max
0.011491
0.0085224
0.0055534
0.0025844
-0.00038459
-0.0033536
-0.0063226
-0.0092916
-0.012261 Min

(a)

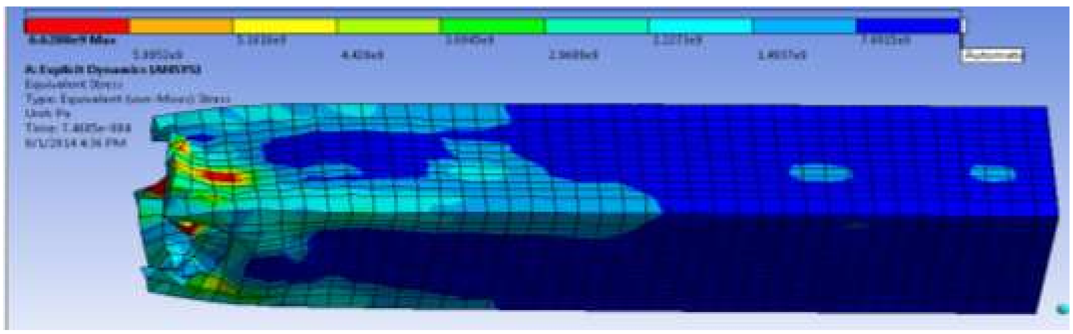

(b)

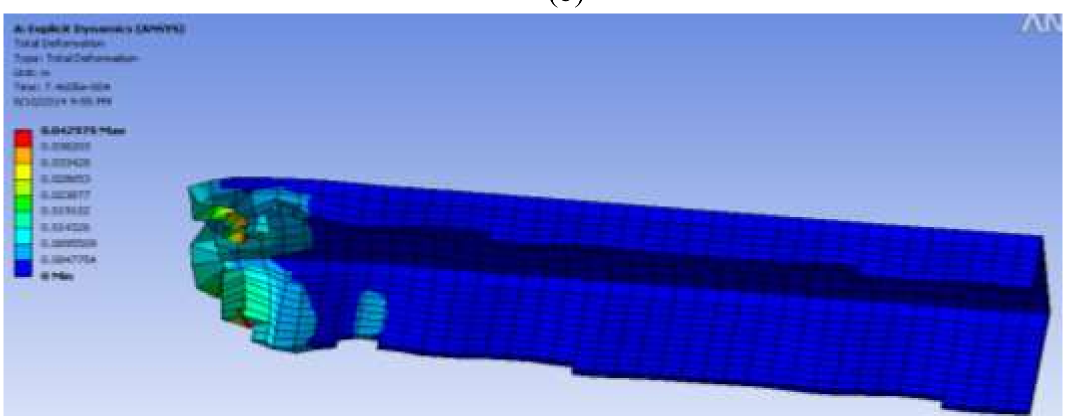

(c)

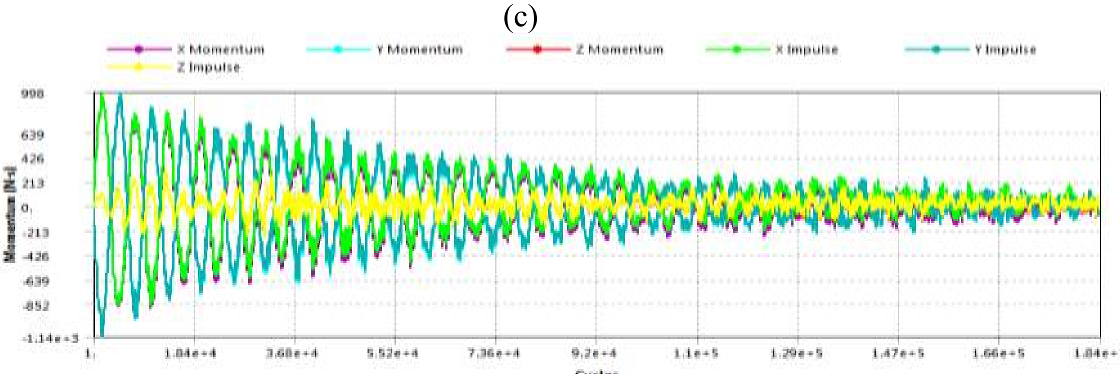
X Momentum
Y Momentum
Z Momentum
X Impulse
Y Impulse
Z Impulse
Momentum [N-s]
998
639
426
213
0.
-213
-426
-639
-852
-1.14e+3
1.
1.84e+4
3.68e+4
5.52e+4
7.36e+4
9.2e+4
1.1e+5
1.29e+5
1.47e+5
1.66e+5
1.84e+5
Cycles

(d)

Figure 5-14 Upper and Lower Energy Absorber (a) Normal elastic strain (b) Equivalent stress (c)Total Deformation (d) Momentum vs. Cycle

Considering for nonlinear analysis the ANSYS LS-DYNA output indicates that the maximum deformation is 0.04298m under impact load of 2000KN for Upper and Lower energy absorber (i.e. Rectangular profile).

5.3 Numerical Results

Let the following notations are used, M_1, M_2 Mass of the vehicle

V_1,V_2 initial speed of the cars ,E_d, Energy to be dissipated in collision

P_{m1}, P_{m2} mean impact force on the vehicle, L_1, L_2, deformation length of the vehicle

a_{a1}, a_{a2}, average acceleration of each vehicle respectively

1. When one locomotive rail vehicle impacts to each other with the same mass and one vehicle standing, i.e.M_1=M_2=40t, V_1=V0, V2=0, mean crushing force (P_m)=2000KN,

Impact Model Equations For Vehicle collides with another Rail vehicle at rest, and having equal Mass and the same material property

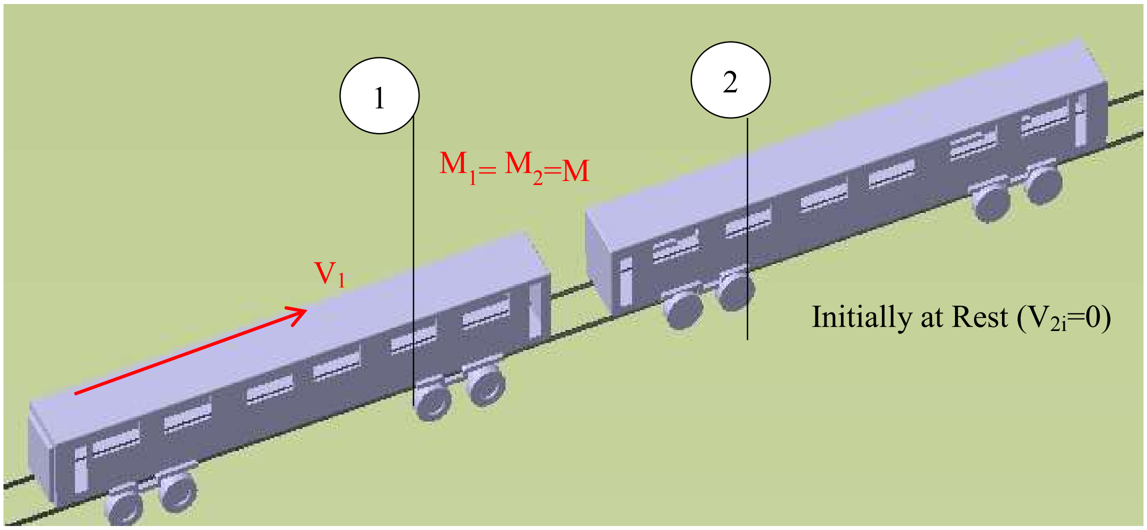

Figure 5-15 Collision between Standing Vehicle.

$$Vf1 = \frac{M1 - M2}{M1 + M2}Vi1 + \frac{2 * M2}{M1 + M2}Vi2$$

But, M_1=M_2=M,

$$Vf1 = Vi2 = 0$$

$$Vf2 = Vi1$$

$$\boldsymbol{Ed = \frac{M*M}{M+M} * \frac{V_0{}^2}{2} = M * \frac{V_0{}^2}{4}} \text{ .... } \mathbf{5\text{-}2}$$

$$\mathbf{L_c} = \boldsymbol{\frac{V_0{}^2}{8*a}} \text{ .... } \mathbf{5\text{-}3}$$

Then the vehicle deformation, energy dissipated average acceleration can be related as:

L_{deform}=V0^2/8*a_a

E_d=M/4*V_0^2

,a_a=F_a/M=2000000/40000=50 m/s^2

Table 5-1 Table Influence of impact velocity on deformation length and kinetic energy dissipated (for two identical Rail Vehicles)

V0(m/s)	Ed(KJ)	Deformation(m)
0	0	0
1	10	0.0025
2	40	0.01
3	90	0.0225
4	160	0.04
5	250	0.0625
6	360	0.09
7	490	0.1225
8	640	0.16
9	810	0.2025
10	1000	0.25
15	2250	0.5625
20	*4000*	*1*
25	6250	1.5625
30(108km/hr.)	9000	2.25
35	12250	3.0625
40	16000	4
45	20250	5.0625
50	25000	6.25

This shows that below 20m/s (72km/hr.) impact velocity the structural performance is piecewise linear response. The maximum deformation length reaches at the impact speed of 108km/hr. which is about 2.25m deformation length. Beyond this speed for this type of collision can result in an intrusion to the passenger compartment and cause high rescue of injuries.

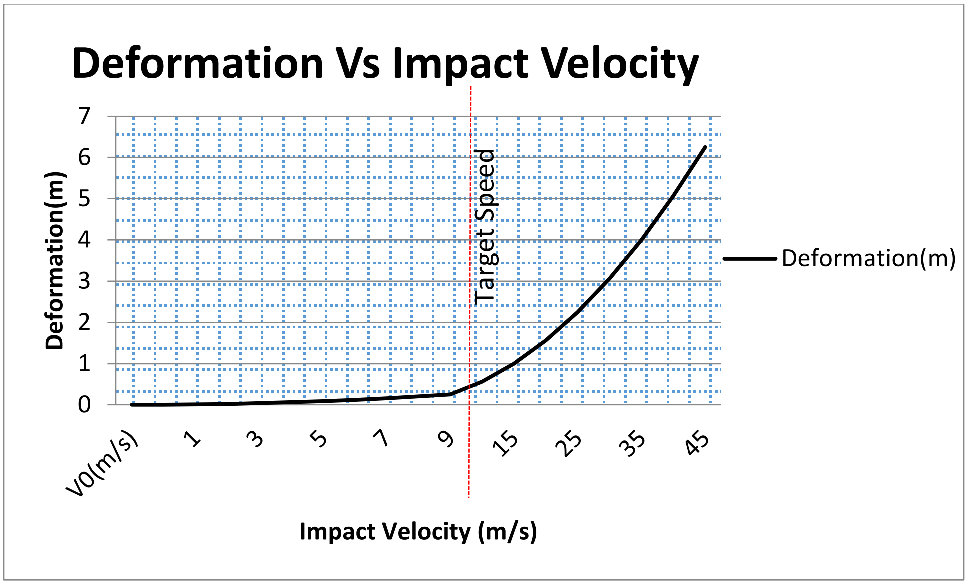

Figure 5-16 Displacement vs. Impact Speed for first Vehicle

The optimum impact speed for this impact condition 72km/hr. under deformation length of 1m. In this situation 4MJ impact energy can absorbed.

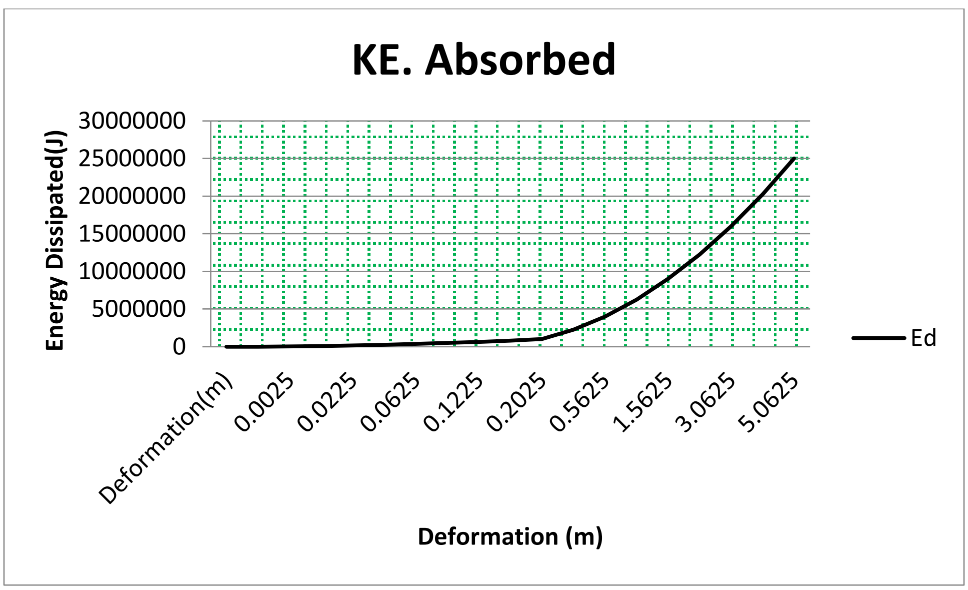

Figure 5-17 Impact energy dissipated vs. deformation

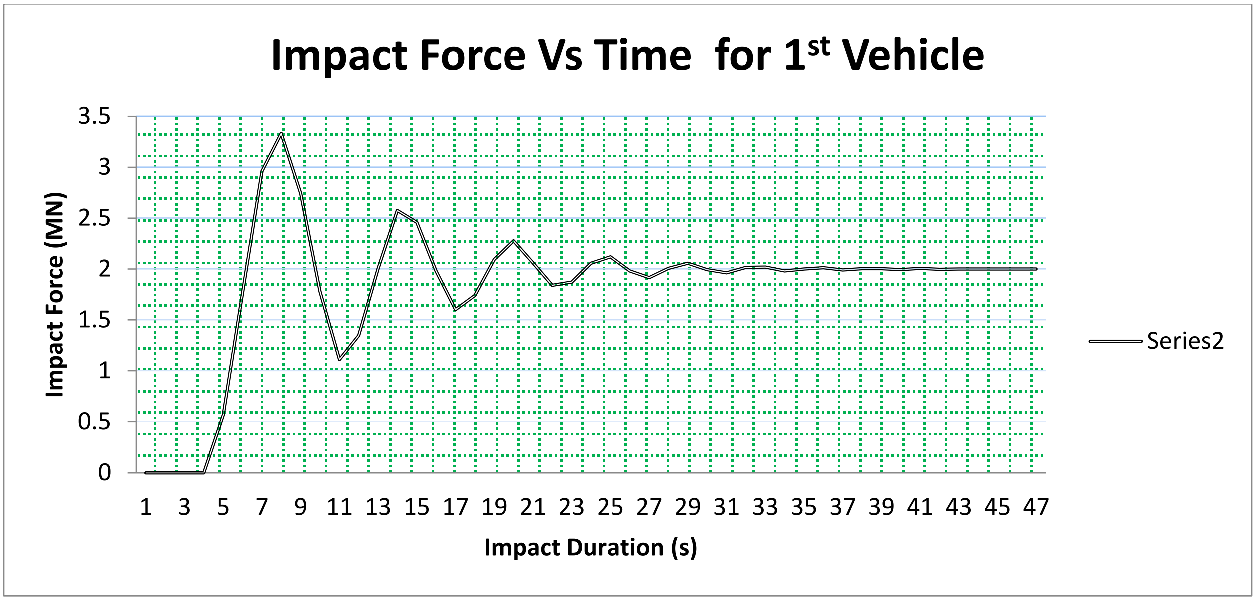

Figure 5-18 Impact force vs. Time graph under 2MN collision Force

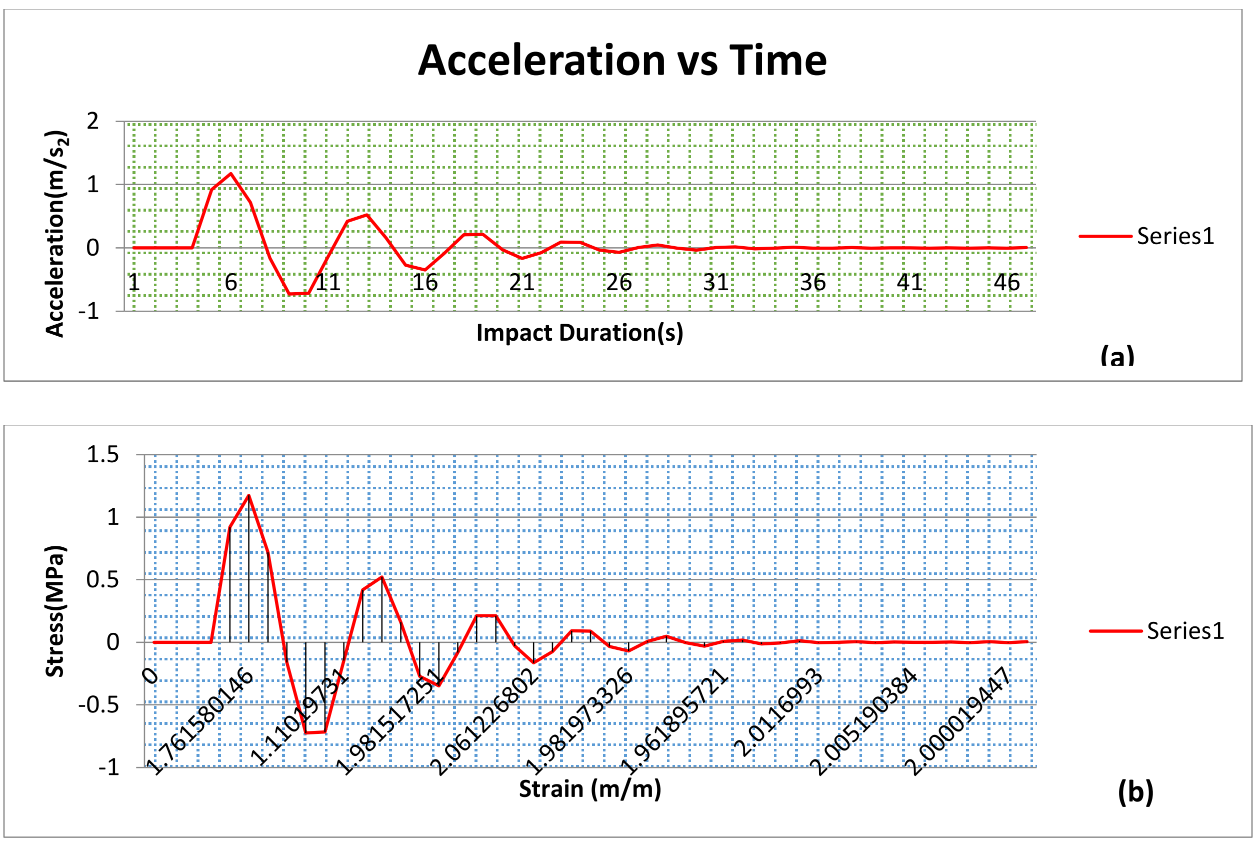

Figure 5-19 (a) Impact Acceleration vs. time under 2MN collision Force (b) Stress vs. Strain

2. When a single rail locomotive impacts to a rigid standing obstacle (wall) i.e. $V1=V0, V_2=0, M_1=M=40t, M_2=\infty$, , mean crushing force $(P_m)=2000KN$

   A. Impact Model Equations For Vehicle collides with Rigid obstacle

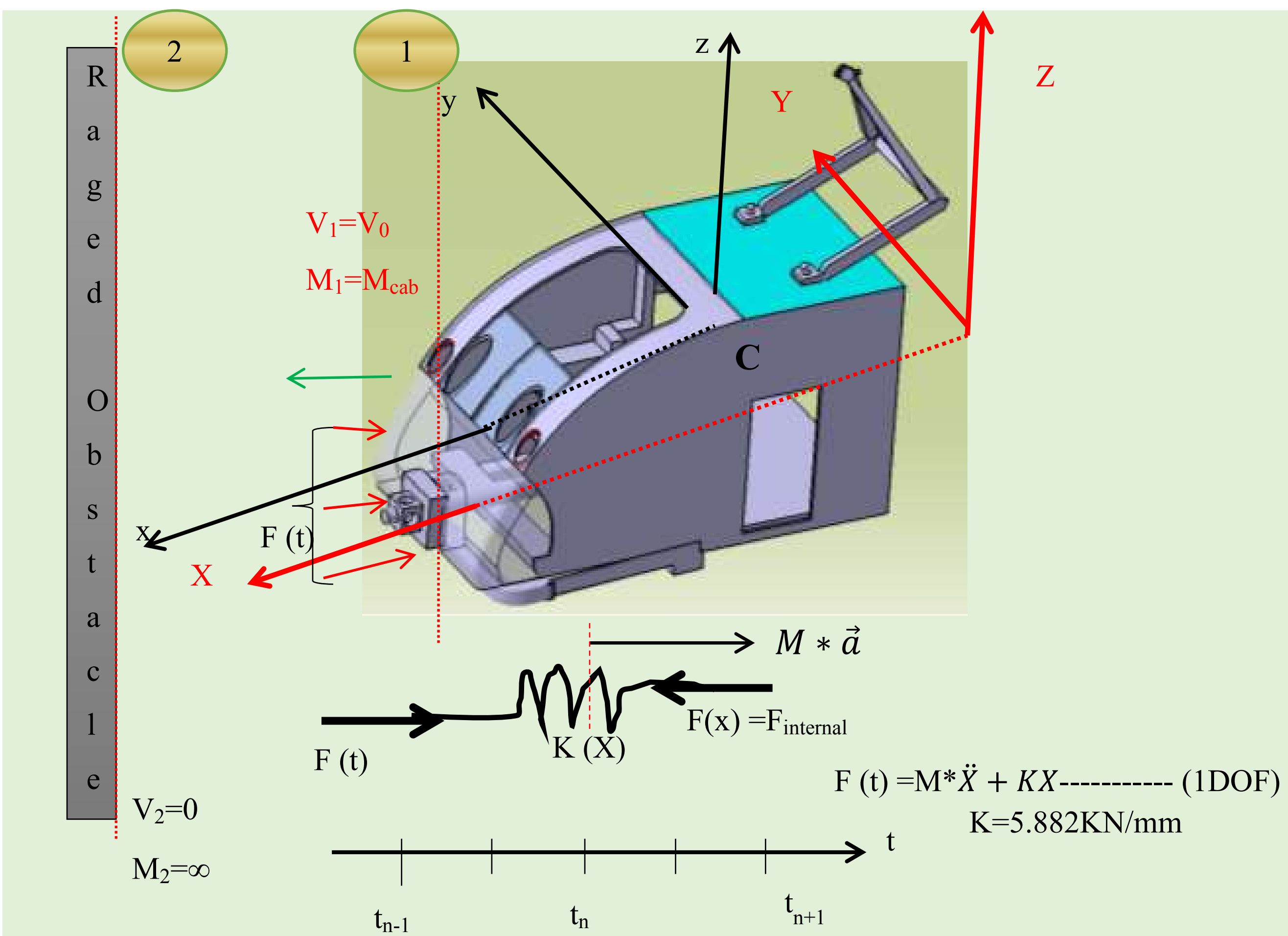

Let, x_n and$(\dot{X})_{n-½}$ be the known quantities, the required quantities are X_{n+1} and $(\dot{X})_{n+½}$. The Dynamic equilibrium at time t_n is expressed

$$\ddot{X}_n = (F_n - KX_n)/M$$

$$\dot{X}_{n+1/2} = \dot{X}_{n-1/2} + \Delta t_n \ddot{X}_n$$

$$X_{n+1} = X_n + \Delta t_{n+\frac{1}{2}}(\dot{X}_{n+\frac{1}{2}})$$

Applying the conservation of the momentum for the system of particles along X axis gives

$\{M_1V_{1x} + M_2V_{2x}\}_{before} = \{M_1V_{1x} + M_2V_{2x}\}_{after}$

Similarly for yaw direction the conservation of momentum yields,

$\{M_1V_{1y} + M_2V_{2y}\}_{before} = \{M_1V_{1y} + M_2V_{2y}\}_{after}$

For $M_2=\infty, V_2=0\ V_1=V_0$

$$Vf1 = \frac{M1 - M2}{M1 + M2} Vi1 \cong -Vi1$$

$KE = \Delta KE_i == \Delta KE_f = E_d$

$$\frac{1}{2}M_1{V_1}^2f - \frac{1}{2}M_1{V_1}^2i = \frac{1}{2}M_2{V_2}^2f - \frac{1}{2}M_2{V_2}^2i$$

$E_d = \frac{1}{2}M * {V_0}^2$ 5-4

$L_c = \frac{{V_0}^2}{2*a}$ 5-5

Table 5-2 Influence of impact velocity on deformation length and kinetic energy dissipated (Vehicle Locomotive impact to rigid obstacle)

V0(m/s)	V0^2	Ed(KJ)	a_{av}	F_{av}	Deformation(m)
0	0	0	50	2000000	0
1	1	20	50	2000000	0.01
2	4	80	50	2000000	0.04
3	9	180	50	2000000	0.09
4	16	320	50	2000000	0.16
5	25	500	50	2000000	0.25
6	36	720	50	2000000	0.36
7	49	980	50	2000000	0.49
8	64	1280	50	2000000	0.64

9	**81**	**1620**	**50**	**2000000**	**0.81**
10	***100***	***2000***	***50***	***2000000***	***1***
15(54km/hr.)	**225**	**4500**	**50**	**2000000**	**2.25**
20	**400**	**8000**	**50**	**2000000**	**4**
25	**625**	**12500**	**50**	**2000000**	**6.25**
30	**900**	**18000**	**50**	**2000000**	**9**
35	**1225**	**24500**	**50**	**2000000**	**12.25**
40	**1600**	**32000**	**50**	**2000000**	**16**
45	**2025**	**40500**	**50**	**2000000**	**20.25**
50	**2500**	**50000**	**50**	**2000000**	**25**

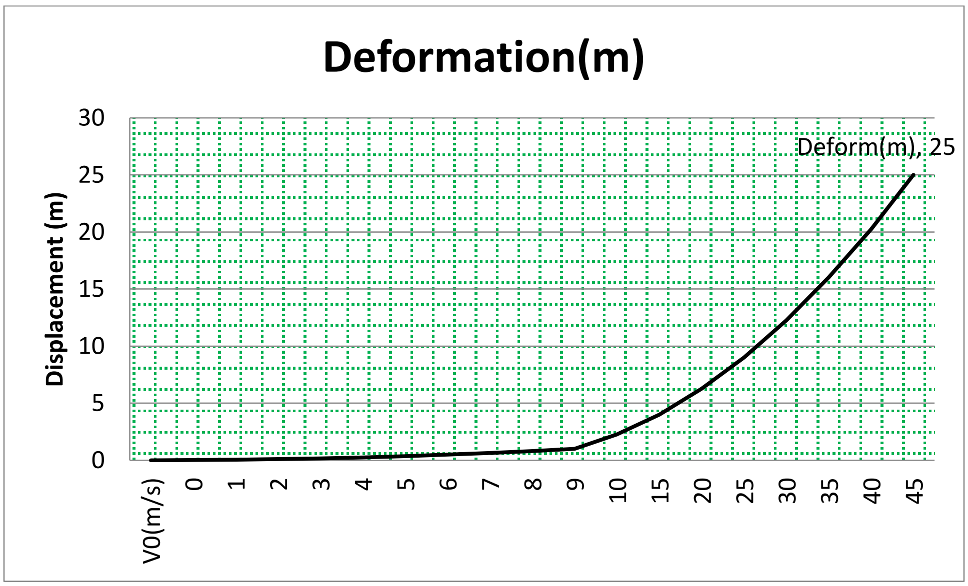

Figure 5-20 Impact Velocity vs. Displacement graph under Rigid body Collision

Based on accident type and normal traveling velocity, the railway vehicle crush zone has been designed. For the passenger rail vehicle having an average mass of 32-40 tons and traveling velocity of 54km/hr. (15m/s).Figure 5-20 shows that the ideal crush zone deformation vs. impact duration curve, in the first step, the frontal nose will be started to deform; then when the load reaches to about 2.5 MN, the main energy absorber will be started to be deformed. After 1.25m deformation of Main energy Absorber both upper and lower energy absorber could started to deform and honeycomb box energy absorber component then be activated. At the final step, when the load reaches to 4.5 MN, sliding sill shearing bolts shall be cut and primary energy absorbers will be activated that absorbs about 2.25MJ energy. At the end of these mechanisms, the total crush zone has been reached and the impact energy beyond 4.5MN can cause compartment intrusion and result in loss of life.

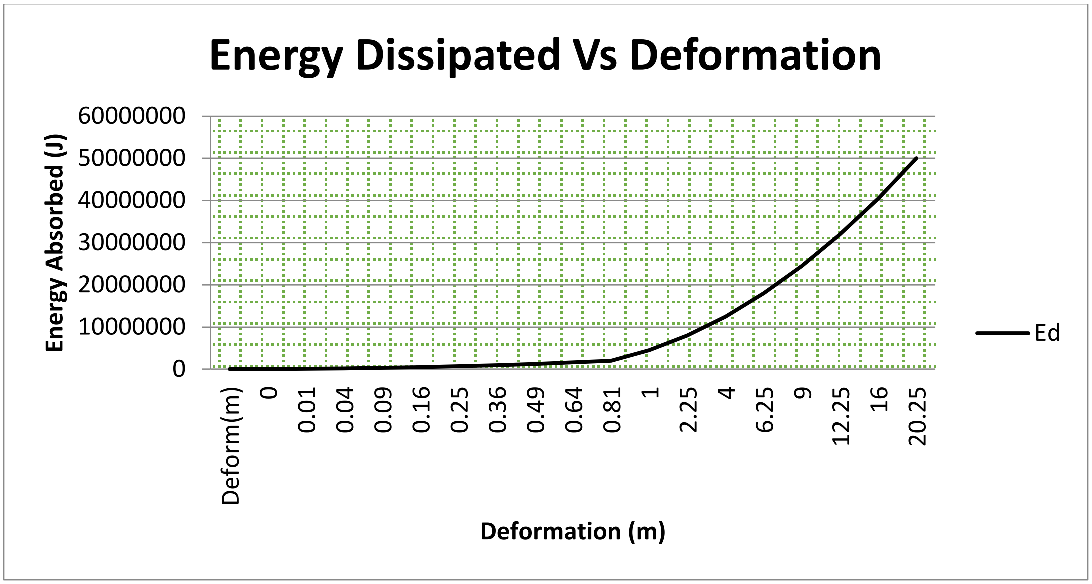

Figure 5-21 Energy Dissipated vs. Deformation for the second situations

This shows that more deformation will result if the vehicle collides with rigid obstacle rather than impacting with each other of identical mass and system structures. When dealing with collision dynamics three levels of harshness of the impact energy can be distinguished.

1. Normal service collision

This is a medium less severity collision where the frontal nose and buffer gears dissipate about 90KJ impact energy.

2. Medium Collision

In medium collision scenarios the crashing elements starts to work. Deformation length of the crashing element is about 1m and the maximum force allowed in the crash-elements amounts to 2000KN. Thus the theoretical amount of energy absorbed is 2MJ. V_0= (20m/s) 72km/hr. for the first case Table5-1 and V_0=10m/s (36km/hr.) for the second case Table 6-2.

3. Strong collision

Under this level the whole crashing zone (i.e. the total deformation is about 2.25m, under the same impact force 2000KN) is involved the plastic deformation process. Thus the theoretical amount of absorbed energy is 4.5MJ and the corresponding rail vehicle impacting velocity is V_0=30m/s (108km/hr.) for the first case, and 15m/s (54km/hr.).

The above impact model shows that the kinetic energy of the vehicle can be absorbed completely at the front end (i.e. Cab structure) of the vehicle. Therefore the construction of the vehicle Driver's cab is very important. These results simplifies the latter simulations requirement because the results coming from a single car model are quite good extendable to a train with a given velocity. But here for its complexities overriding effect, derailments, etc. are neglected.

CHAPTER-6

6 CONCLUSION AND RECOMMENDATION

6.1 Conclusion

The main crush worthiness components of Rail vehicle cab is the two substantial welded steel Supporting ***pillars***. These provide cab's overall static and Dynamic Strength. They also resist the collapse loads of the other thin walled tubes of crushing element such as Main energy absorber and upper, lower energy absorber components.

In this report the performance of the selected thin walled profiles, rectangular, circular, etc. have been evaluated and the result shows that Octagonal profile can absorb more impact energy than the other.

In-line frontal collisions are analyzed and the results are within the standard requirements.

As a result, it has been shown that it is possible to design a rail vehicle's cab body structure taking *crashworthiness* into account, and On the other hand it is also possible to design *crash safety* structure taking the into account by means of structural dynamic simulation.

6.2 Recommendation

In modern LRT rail vehicle cab it is required for **structural comfort**; **crash worthiness enhancement**, good **aerodynamic and ergonomic consideration**, within a single integrated cab profile.

Compared to the existing Rail vehicle Cab this cab is lighter, simple, has fewer parts, and less expensive.

Longitudinal deformation must be less stiff than the side deformation (damping KE without roll over problem).

This can be done by decreasing the wall thickness and density variation of the Crushing Element through its length.

6.3 Future Work

Human life is priceless. This research considers only inline frontal collision of the rail vehicle cab. Thus offset (deviation from center of mass), side impact as well as roll-over impact dynamic simulations are required for its application. In another way this paper is only based on computational impact simulation scenarios, from practical perspective it is required to test the model practically.

For optimization of crush worthiness structure the material model is also required, to model. Material strain rate and thermal effect should be tested numerically.

APPENDIX A. IMPACT MODEL AMENDMENT

Principles of Dynamics

The momentum of an object is the product of its velocity and mass. It is a vector quantity and points in the same direction as the velocity vector.

- Newton's Second Law can be phrased more generally as the force equaling the time derivative of the momentum.
- The change of momentum, impulse, is the time integral of the force that causes the momentum change.
- In all collisions, the total momentum is conserved. The law of the conservation of momentum is the second conservation law that we encounter, after the law of energy conservation.
- Besides momentum conservation, totally elastic collisions also have the property that the total kinetic energy is conserved.
- In totally inelastic collisions, the maximum amount of kinetic energy is removed, and the colliding objects stick to each other. Total kinetic energy is not conserved, but total momentum is.
- All cases in between these two extremes are partially inelastic, and the change in kinetic energy is proportional to the square of the coefficient of restitution.

Momentum Linear momentum (not angular) is the product of the mass and it's Velocity

$$\vec{p} = M * \vec{V}$$

As it can be seen, lowercase letter p is the notation for momentum. The velocity is a vector; and we multiply this vector by a scalar quantity, the mass M. The product is then a vector as well. The momentum vector, p, and the velocity vector, are parallel to each other.

Momentum and Force

$$\mathbf{F=m*a=}\boldsymbol{M} * \frac{\boldsymbol{dV}}{\boldsymbol{dt}}=\frac{\boldsymbol{d}}{\boldsymbol{dt}}\vec{p}$$

$$\mathrm{F}=\frac{\boldsymbol{d}}{\boldsymbol{dt}}\vec{p}$$

Momentum and Kinetic Energy

$$KE = \frac{1}{2}M * V^2 = \frac{1}{2M}M^2 * V^2 = \frac{1}{2M}p^2$$

Impulse (J) is the change in Momentum, (or time integral of Force)

$$J=\Delta p=\int_{t1}^{t2} Fdt$$

$$F_{av}=\frac{\int_i^f Fdt}{\int_i^f dt} = \frac{1}{tf-ti}\int_i^f Fdt = \frac{J}{\Delta t}$$

$$J=F_{av}\Delta t$$

For Totally elastic collision the momentum is conserved

i.e. $p_{1i}+p_{2i}= p_{1f}+p_{2f}$

$$\frac{1}{2M1}p^2f - \frac{1}{2M1}p^2i = \frac{1}{2M2}p^2f - \frac{1}{2M2}p^2i$$

Putting for p=M*V and rearranging the equation gives

$$Vf1 = \frac{M1 - M2}{M1 + M2}Vi1 + \frac{2 * M2}{M1 + M2}Vi2$$

$$Vf2 = \frac{M2 - M1}{M1 + M2}Vi2 + \frac{2 * M1}{M1 + M2}Vi1$$

Special Cases

1. *When the impacting vehicle have the same mass, then*

$$Vf1 = Vi2$$

$$Vf2 = Vi1$$

2. *When one of the impacting vehicle is initially at rest then,*

$$Vf1 = \frac{M1 - M2}{M1 + M2}Vi1$$

$$Vf2 = \frac{2 * M1}{M1 + M2}Vi1$$

APPENDIX B. PROJECT WORK SCHEDULES /GANT CHART

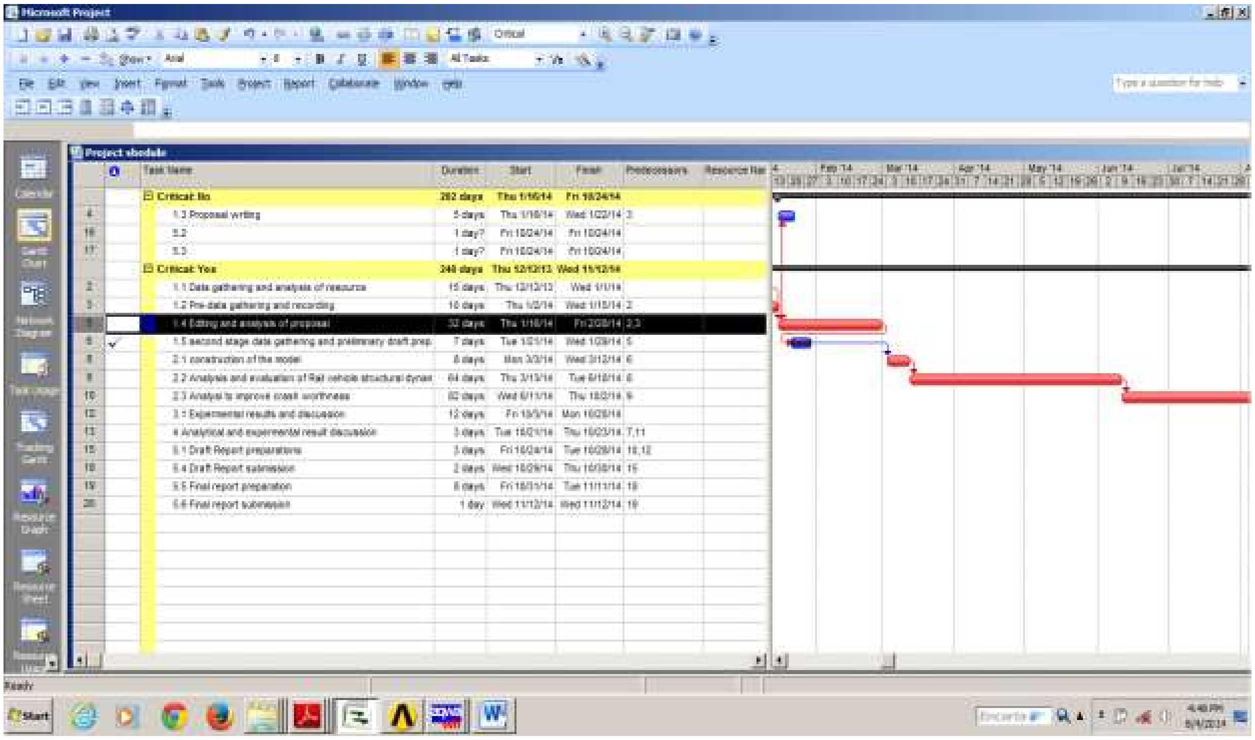

Gant Chart Schedule for the thesis project

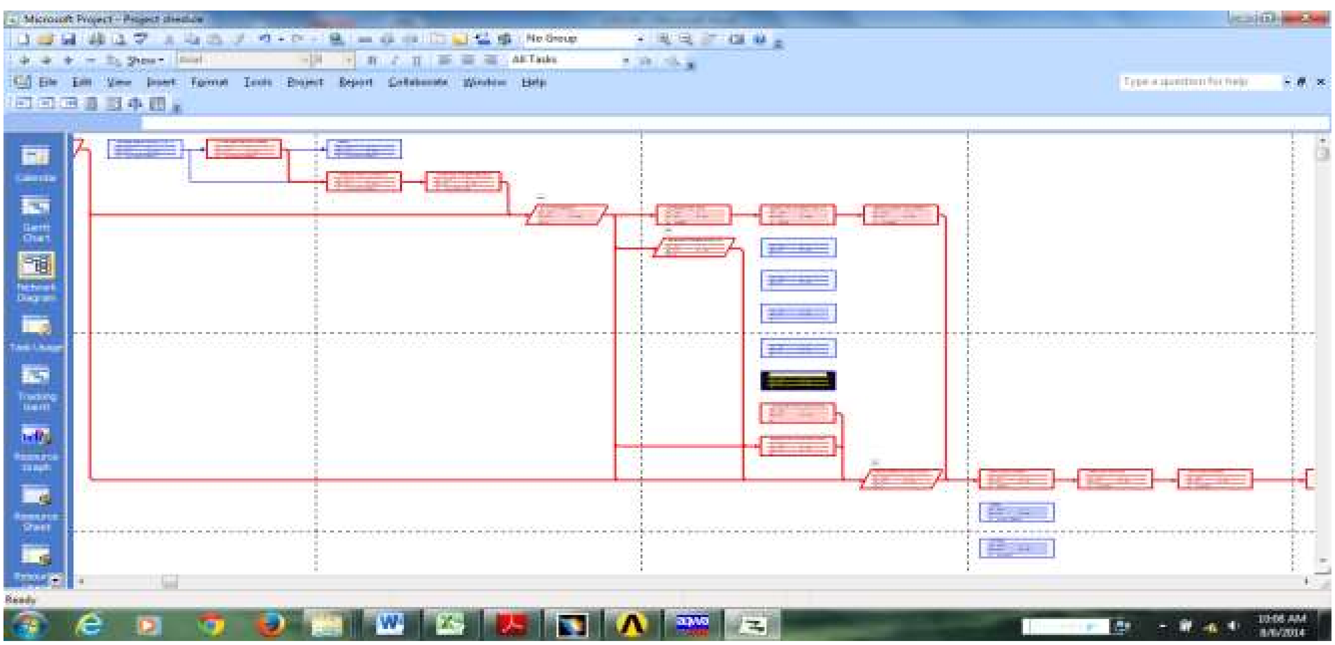

Critical path and critical activities

7 REFERENCES

1. Taylor and Francis, Handbook of railway vehicle dynamics / Simon Iwnicki. p. cm. ISBN-13: 978-0-8493-3321-7 Railroads--Cars--Dynamics--Handbooks, manuals, etc. I. Iwnicki, S. (Simon), 1962- TF550.H37 2006
2. R. Happee, A. Janssen, E. Fraterman, J. Monster, and R. Happee, "Application of MADYMO Occupant Models in LS-DYNA/MADYMO Coupling," in 4th European LS-DYNA Users Conference, 2003.
3. W. Abramowicz and N. Jones, "Dynamic axial crushing of square tubes," International Journal of Impact Engineering, 1984.
4. A. Schoofs, M. Klink, and D. van Campen, "Approximation of structural optimization problems by means of designed numerical experiments," Structural and Multidisciplinary Optimization, 1992.
5. Canadian motor vehicle safety regulations May 2009
6. "European regulations related to crash testing, network.com/regulations/ece-regulations/ece-regulations.html," accessed on May 2009.
7. Design Optimization of Vehicle Structures for Crashworthiness Improvement , Hesham Kamel Ibrahim A Thesis in Partial Fulfillment of the Requirements For the Degree of Doctor of Philosophy at Concordia University ontreal, Quebec, Canada August 2009
8. Modelling and Analysis of the Crush Zone of a Typical Australian Passenger Train Cooperative Research Centre (CRC) for Rail Innovations, Australia (http://eprints.qut.edu.au/52047/)
9. Light weight Composite Rail Driver's Cab. Conor O'Neill Rail Vehicles Group Manager, NewRail
10. Light Rail Technology Hamilton Public work (April 2009)
11. . A review of Impact models for vehicle collisions. R. Mattew Brach. Triodyne.inc.Vol. No.870048
12. Witold Pawlus, Hamid Reza Karimi, and Kjell G. Robbersmyr. Reconstruction and simulation of the vehicle to road safety barrier oblique collision based on the levenberg-marquardt algorithm. International Journal of Crashworthiness, 17(6):676{692, 2012.

doi:10.1080/13588265.2012.714300.URL http://www.tandfonline.com/doi/abs/10.1080/13588265. 2012.714300.

13. R.N. Jazar. Vehicle Dynamics: Theory and Application. Springer, 2008. ISBN 9780387742434.URL http://books.google.no/books?id=Pvsv78xj7UIC.
14. Computer-Aided Analyses of Vehicle Structures. Thomas Jin-Chee Liu Taiwan Feb. 2009
15. Impact Tests of Crash Energy Management Passenger Rail Cars: Analysis and Structural Measurements. November 13-19, 2004, Anaheim, CA, IMECE2004-61252
16. C. L. Magee, "Design for crash energy management, present and future developments," in Seventh International Conference on Vehicle structural mechanics, (Detroit, Michigan, USA), 1988.
17. H. F. Mohamed and B. B. Fileta, Design of vehicle structures for crash energy management, pp. 11–110. Vehicle Crashworthiness and Occupant Protection, American Iron and Steel Institute, 2004.
18. B. Deshpande, T. J. Gunasekar, R. Morris, S. Parida, M. Rashidy, and S. Summers, "Methodology development for simulating full frontal and offset frontal impacts using full vehicle MADYMO models," ASME Applied Mechanics Division Publications AMD 237, pp. 19–38, 1999.
19. R. T. Shea and J. Kral, "Madymo simulations of occupant and vehicle kinematics in offset and oblique barrier tests," ASME Conference Proceedings, pp. 419–426, 2005.
20. E. Haug, F. Arnaudea, J. Du Bois, and A. Rouvay, "Static and dynamic finite element analysis of structural crashworthiness in automotive and aerospace industries," Structural Crashworthiness, pp. 175–217, 1983.
21. C. D. Kan, D. Marzougui, G. T. Bahouth, and N. E. Bedewi, "Crashworthiness Evaluation Using Integrated Vehicle and Occupant Finite Element Models,"International Journal of Crashworthiness 6(3), pp. 387–398, 2001.
22. H. Zhang, "Evaluation of frontal occupant protection system responses to crash pulse variations," International Journal of Crashworthiness 11(3), pp. 243–250, 2006.
23. J. Wu, Crashworthiness simulation of roadside safety structures with development of material model and 3-D fracture procedure. PhD thesis, University of Cincinnati, 2000.

24. H. A. Whitworth, R. Bendidi, D. Marzougui, and R. Reiss, "Finite element modeling of the crash performance of roadside barriers," International Journal of Crashworthiness 9, pp. 35–43, 2004.
25. A. O. Atahan and M. ASCE, "Finite-Element Crash Test Simulation of New York Portable Concrete Barrier with I-Shaped Connector," Journal of Structural Engineering 132, pp. 430–440, 2006.
26. J. Yang, "Pedestrian head protection from car impacts," International Journal of Vehicle Design 32, pp. 16–27, 2003.
27. "Design, fabrication and testing of a component hic tester for aircraft applications," International Journal of Crashworthiness 10(5), pp. 515–524, 2005.
28. J. Wismans, Design tools: Human body modeling, pp. 227–268. Vehicle crash worthiness and occupant protection, Michigan: American Iron and Steel Institute, 2004.
29. R. R. McHenry, "Analysis of the Dynamics of Rail Vehicle Passenger-Restraint Systems," in Stapp Rail vehicle Crash and Field Demonstration Conference, pp. 207–248, 1963.
30. M. Iwamoto, Y. Kisanuki, I. Watanabe, K. Furusu, K. Miki, and J. Hasegawa, "Development of a Finite Element Model of the Total Human Model for Safety (THUMS) and Application to Injury Reconstruction," in Proceedings of the 2002 IRCOBI International Conference The BRIDGE, pp. 31–42, 2002.
31. Grzegorz Brożek and Tadeusz Uhl. Explicit FEM in analysis of crash elements. 9–12 May 2011, Warsaw, Poland
32. International Journal of Scientific & Engineering Research, Volume 4, Issue 8, August 2013 ISSN 2229-5518
33. ANSYS Mechanical APDL Tutorials Release 13 November 2010.
34. Training@PredictiveEngineering.com LS-DYNA® Analysis for Structural Mechanics.